Review

Structure And Dynamic States of Actin Filaments

Dorit Hanein and Niels Volkmann *

Posted Date: 29 April 2026

doi: 10.20944/preprints202604.2036.v1

Keywords: actin; cytoskeleton; actin filaments; ATP hydrolysis; actin binding proteins; Cryo-EM; structural dynamics; actin isoforms; cell motility; polymerization; in situ structural biology

 doi:10.20944/preprints202604.2036.v1

Review

Structure And Dynamic States of Actin Filaments

Dorit Hanein [1] and Niels Volkmann [2,*]

[1] Department of Bioengineering, Department of Chemistry and Biochemistry, University of California, Santa Barbara, CA 93106, USA

[2] Department of Bioengineering, Department of Electrical and Computer Engineering, Program for Interdisciplinary Quantitative Biosciences, University of California, Santa Barbara, CA 93106, USA

* Correspondence: nvo@ucsb.edu

Abstract

Actin, a highly conserved and ubiquitous eukaryotic protein, underlies essential cellular processes including motility, shape maintenance and muscle contraction. Its dynamic transition between monomeric and filamentous states is powered by ATP hydrolysis, which undergoes structural rearrangements that accelerate turnover in filaments and serve as a measure of filament aging. A wide range of actin binding proteins (ABPs) regulate polymerization, depolymerization, and network organization. Recent high resolution cryo-EM and cryo-ET studies have revealed detailed structures of actin, its isoforms, and ABP complexes, including their organization in cells, deepening our understanding of actin function in health and disease.

Keywords: actin; cytoskeleton; actin filaments; ATP hydrolysis; actin binding proteins; Cryo-EM; structural dynamics; actin isoforms; cell motility; polymerization; in situ structural biology

1. Introduction

The actin molecule is an evolutionarily ancient and conserved protein found across all eukaryotic life forms (Hightower and Meagher, 1986). The actin gene originated in the common ancestor of all lifeforms as evidenced by the fact that bacteria, archaea, and eukaryotes all have actin-like molecules related structurally and functionally to each other (Gunning et al., 2015b). All eukaryotes have one or more genes for actin, and sequence comparisons have established that they are one of the most conserved gene families, varying by only a few amino acids between algae, amoeba, fungi, and humans. Actin is one of the most abundant proteins on Earth and the most abundant protein in many cells, often accounting for 10% or more of total protein (Pollard, 2016). It constitutes one of the three principal cytoskeletal polymers, capable of reversibly assembling into dynamic filaments. Actin is essential for numerous fundamental cellular processes, including intracellular transport, cellular structure and motility, muscle contraction, and cytokinesis (Dominguez and Holmes, 2011). Evolution has produced a system of proteins that utilize actin monomers along the filaments to construct diverse cellular structures, from the stable sarcomeres of striated muscles to the rapidly remodeling, force-generating branched networks found at the leading edges of motile cells that turn over within seconds. Understanding the structure of the actin molecule is essential for deciphering its functional properties, including its polymerization dynamics and the regulatory mechanisms mediated by these actin-binding proteins (ABPs).

Actin primarily exists in two interconvertible structural forms: the monomeric, globular G-actin, and the polymeric, filamentous F-actin. The G-actin polypeptide, comprising 375 amino acid residues with a molecular weight of approximately 42 kDa, folds into a relatively flat protein (Figure 1A) characterized by a deep medial cleft (Kabsch et al., 1990). This cleft serves as the nucleotide-binding pocket, where ATP binds and gets hydrolyzed. The actin monomer is typically described as possessing four subdomains (SD1, SD2, SD3, and SD4), with the polypeptide chain winding from the amino N-terminus in subdomain 1, through subdomains 2, 3, and 4, and returning to subdomain 1

 doi:10.20944/preprints202604.2036.v1

at the carboxyl terminus. A notable "target-binding cleft" exists between subdomains 1 and 3, serving as a central site for interactions with various proteins (Dominguez, 2004). Despite significant variations in bound molecules or nucleotide states, the conformation of the actin monomer remains largely consistent. Actin is also part of a larger structural superfamily that includes Actin-Related Proteins (ARPs), sugar kinases, hexokinases, Hsp70 proteins, and even prokaryotic actin-like proteins such as MreB and ParM (Stoddard et al., 2017). The N-terminal methionine and cysteine residues of the actin polypeptide are acetylated and cleaved, with the resulting N-terminal aspartic acid then reacetylated (Rebowski et al., 2020).

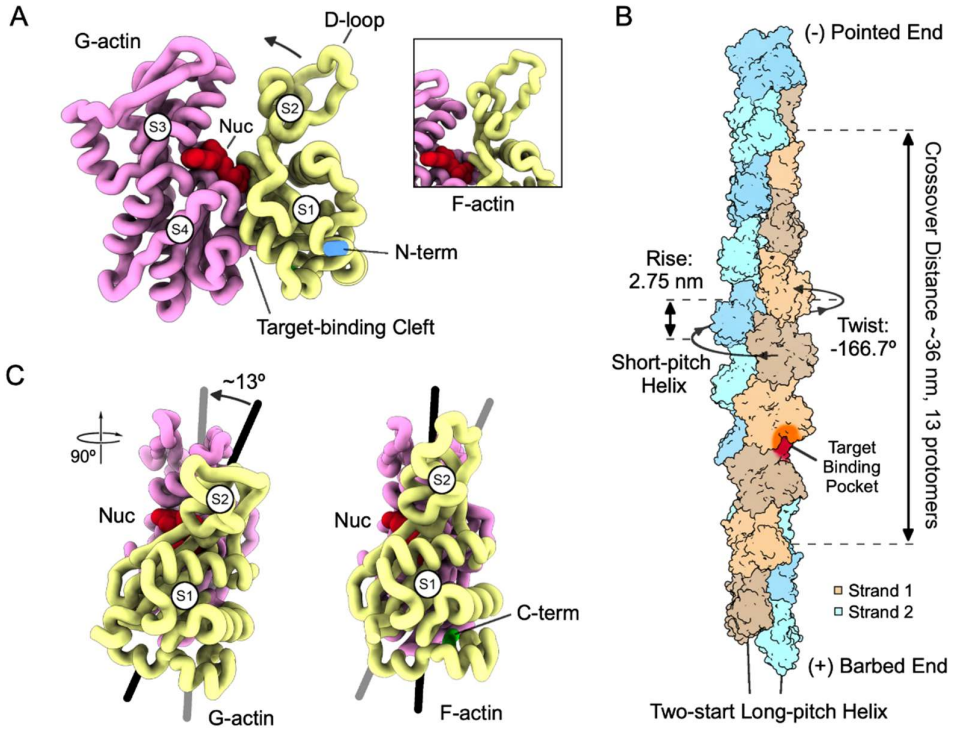

Figure 1. *Actin in Its Monomeric and Filament Forms.* (A) Structure of globular (G-actin) monomer showing the four subdomains (SD1–SD4), the nucleotide (Nuc, red), the N-terminus (N-term, blue), the DNase-binding loop (D-loop), and the target-binding cleft. The rearrangement of the D-loop upon filament formation (arrow) is shown in the inset. (B) Geometry and features of the filamentous (F-actin) form. The target-binding pocket, formed by the target-binding cleft of one protomer (orange) and the D-loop of its long-pitch neighbor (red), is highlighted. (C) Transition from G-actin to F-actin. Subdomains SD1 and SD2 are colored yellow, SD3 and SD4 in pink, the C-terminus (C-term) in green, and the nucleotide (Nuc) in red. This view is rotated 90° relative to panel A. The propeller-like flattening of the molecule during filament formation is indicated by lines and arrows.

Upon polymerization, G-actin transforms into F-actin, a polar, helical polymer with distinctly identifiable "barbed" (+) and "pointed" (–) ends (Figure 1B). This polarity is historically evident from the "arrowheads" formed by myosin subfragment-1 binding, which provide a clear directional orientation under electron microscopy (Huxley, 1963). The transition from G-actin to F-actin involves significant structural rearrangements, primarily a 13° propeller-twist of the outer domain relative to the inner domain (Figure 1C), essentially flattening F-actin with respect to G-actin (Holmes et al., 1990). This flattening enables stable inter-subunit contacts within the filament, particularly the insertion of the D-loop (a flexible region in monomers, spanning residues 40-50 in SD2) into the target-binding cleft of the adjacent subunit. Together with the remaining accessible parts of the target binding cleft, the D-loop provides a common binding site for many ABPs (McGough, 1998). While the D-loop often adopts a "closed" state in F-actin, it is generally dynamic in nature (Durer et al.,

 doi:10.20944/preprints202604.2036.v1

2012), and its conformational state and stability are sensitive to the bound nucleotide, applied mechanical forces, and interactions with ABPs.

The F-actin filament is characterized by its helical geometry: each subunit is related to its neighbor by a rotation of approximately 167° about the helix axis in a left-handed sense and a translation along the axis of 27.5 Å (Figure 1B). The helical structure reveals 13 molecules repeating in almost exactly six left-handed turns. F-actin also displays inherent structural flexibility and variability in its helical twist and rise (Egelman et al., 1982), which can be influenced by its nucleotide state, bound ABPs, and mechanical forces. F-actin's bending persistence length is approximately 11 μm (Gittes et al., 1993), and the torsional persistence length ranges from 8 to 13 μm (Tsuda et al., 1996).

The dynamic behavior of actin filaments is profoundly influenced by their bound nucleotide, which is either ATP, ADP, or ADP.Pi (ADP plus inorganic phosphate). Generally, monomeric G-actin has a bound ATP, whereas most subunits within a filament have a bound ADP. The reason is that ATP hydrolysis occurs extremely slowly in monomeric G-actin but is dramatically accelerated by over four orders of magnitude when actin is incorporated into filamentous F-actin (Korn et al., 1987). ATP hydrolysis into ADP.Pi and the subsequent release of inorganic phosphate (Pi) are the key drivers of actin filament turnover (Pollard, 1986). While Pi release from the F-actin core is relatively slow, it is orders of magnitude faster at the barbed end (Melki et al., 1996). Ultimately *in cellulo*, the control over the dynamic assembly and disassembly of actin filaments is orchestrated by a large and diverse set of ABPs (Pollard, 2016). These proteins fine-tune virtually every aspect of actin dynamics. Actin filaments in cells typically range from a little less than 100 nanometers to a few microns in length (Podolski and Steck, 1990), with their size tightly regulated by actin-binding proteins and cellular context (Fowler, 1996).

Despite decades of research following actin's discovery in the 1940s (Rall, 2018), the molecular mechanisms underlying actin filament dynamics remained poorly understood for much of the twentieth century. A major limitation was the inaccessibility of high-resolution structural information, as actin filaments are not amenable to crystallization. Recent transformative advancements in cryogenic electron microscopy (cryo-EM) have overcome this barrier, enabling researchers to directly image actin filaments and unravel their dynamic regulation with near-atomic resolution (Oosterheert et al., 2025). Many of these structural studies have relied primarily on actin purified from mammalian skeletal muscle, a long-standing source of high-quality protein (Heissler and Chinthalapudi, 2025), but progress in expression systems (Ceron et al., 2022; Haarer et al., 2023) has recently enabled studying the structural impact of human isoform differences (Arora et al., 2023) and disease-causing mutations (Ceron et al., 2024; Huang et al., 2024).

However, within cells, actin behavior differs dramatically from that of its purified protein. Although actin is among the most conserved proteins across eukaryotes, its dynamics in vivo are intricately controlled by more than 160 known ABPs (Meenakshi S et al., 2023). These proteins coordinate key processes such as polymerization, depolymerization, capping, severing, bundling, and cross-linking of actin filaments. In vitro, actin rapidly polymerizes above the critical concentration and forms relatively stable filaments with slow turnover. In contrast, in cells, despite actin concentrations far above the critical threshold (approximately 25 to 100 micromolar) about half remains unpolymerized, and filaments turnover in tens of seconds (Pollard, 2016). This rapid remodeling is driven by the regulatory actions of ABPs, which maintain dynamic monomer pools and organize diverse cytoskeletal architectures to support processes such as motility, adhesion, intracellular transport, and membrane remodeling. Many ABPs are multifunctional and interact with actin-associated proteins, adding layers of spatial and temporal regulation responsive to cellular cues (Lappalainen, 2016).

High-resolution structural insights have been instrumental in elucidating the molecular basis of actin regulation. Yet, fully understanding actin function especially its coordination with ABPs, requires visualization in the native cellular environment, where molecular interactions are precisely integrated with physiological context. Recent advances in cryogenic electron tomography (cryo-ET)

 doi:10.20944/preprints202604.2036.v1

have made it possible to study actin assemblies within intact cells in three dimensions at nanometer resolution (Schneider and Jasnin, 2024). When combined with cryogenic correlative light and electron microscopy (cryo-CLEM), these tools now enable researchers to link actin cytoskeletal architecture to dynamic processes observed in live cells (Hanein and Volkmann, 2024).

Beyond fundamental cell biology, these insights have significant implications for human health. For example, mutations in smooth muscle γ-actin are a common cause of visceral myopathies, a group of rare, severe diseases affecting smooth muscle function in organs like the bowel, bladder, and uterus (Ceron et al., 2024). Other actin mutations have been associated with diffuse large B cell lymphoma and multiple myeloma (Witjes et al., 2020), and dysregulation of actin dynamics and ABP function is a hallmark of cancer cell invasion and metastasis (Yamaguchi and Condeelis, 2007). Together, these findings highlight that a deep understanding of actin structure and its regulation by binding partners is essential for elucidating cellular physiology as well as addressing a wide spectrum of human diseases.

2. Structural Mechanisms of Actin Filament Aging and ATP Hydrolysis

The ability of G-actin monomers to self-organize into filaments, that elongate and disassemble is highly intertwined with their capacity to couple conformational plasticity with ATP hydrolysis. Actin filaments are primarily regulated by ABPs, but the intrinsic aging of F-actin, defined by the sequential transition from ATP to ADP.Pi and finally to ADP (Wegner, 1976), emerges from structural changes encoded in the actin polymer itself.

2.1. ATP hydrolysis

ATP hydrolysis is inefficient in G-actin monomers, which display negligible ATPase activity (~7×10^{-6} s^{-1}). Upon polymerization, however, the rate of hydrolysis increases by more than 40,000-fold (McCullagh et al., 2014; Merino et al., 2020). This dramatic activation is achieved through conformational rearrangements of the F-actin subunit (Figure 1C), wherein the outer domain (comprising SD1 and SD2) rotates relative to the inner domain (SD3 and SD4), bringing the two halves of the nucleotide-binding cleft into closer proximity (Oda et al., 2009; Merino et al., 2018; Chou and Pollard, 2019).

At the heart of this reorganization lies a catalytic triad consisting of residues Q137, D154, and H161 which coordinate and position a water molecule (W_{nuc}) for nucleophilic attack on the γ-phosphate (Figure 2A). In the G-actin state, Q137 and H161 are relatively distant from the nucleotide (Kanematsu et al., 2022). While W_{nuc}, is hydrogen-bonded to Q137, it is not close enough or at the correct angle to perform a nucleophilic attack on ATP.

 doi:10.20944/preprints202604.2036.v1

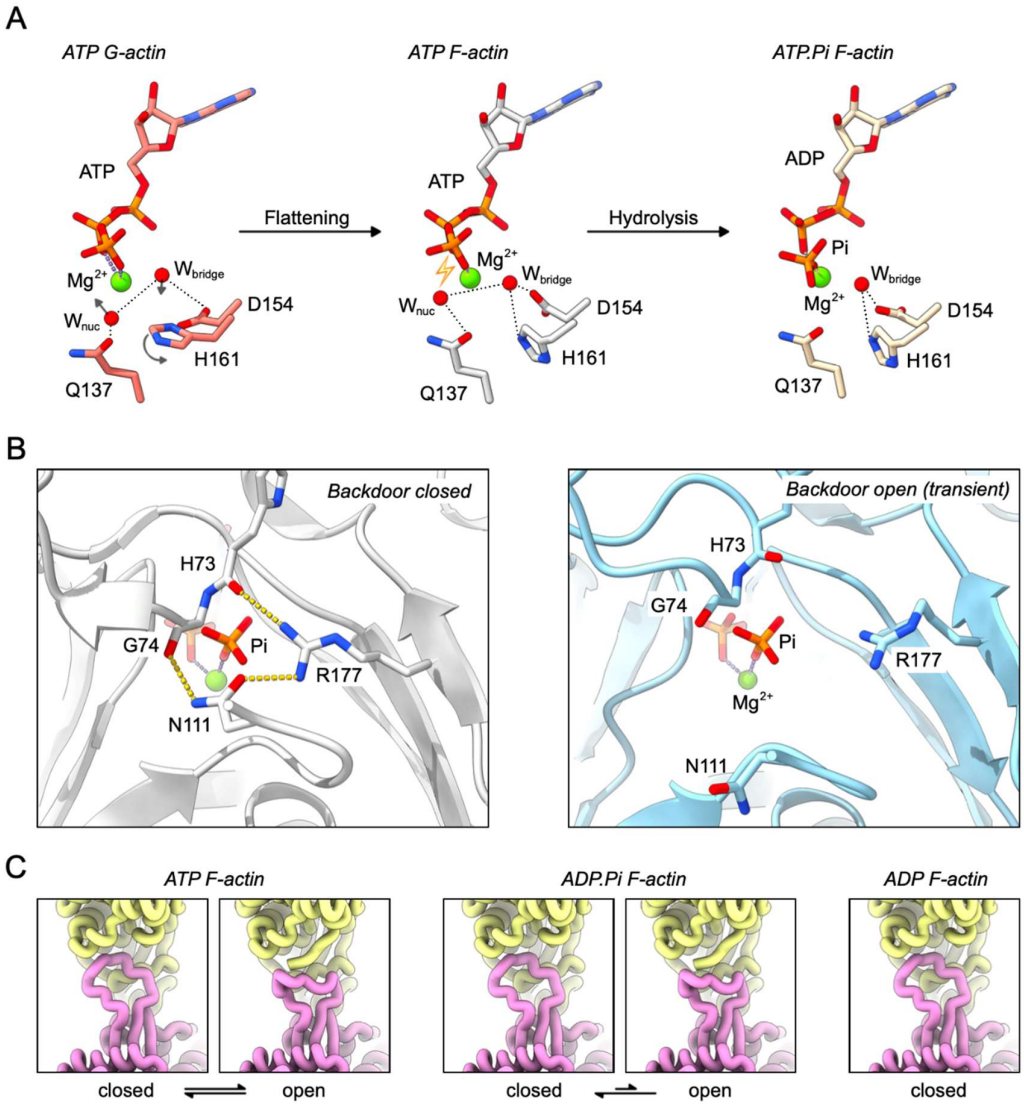

Figure 2. ***Mechanism and effect of ATP hydrolysis.*** A. Rearrangements in the nucleotide-binding pocket during polymerization (flattening) and ATP hydrolysis. Flattening induces a structural rearrangement (arrows) that facilitates the formation of a crucial hydrogen-bonding network (dashed lines) involving residues Q137, D147, H161 and a bridging water (W_{bridge}). This network activates a second water molecule (W_{nuc}), hydrogen-bonded to Q137, for nucleophilic attack (lightning bolt) on ATP. The ATP-F-actin state is modeled after the ADP.BeF_3-F-actin structure. B. View of the nucleotide-binding pocket from inside the filament, highlighting the hydrogen-bonding network (yellow dashed lines) that stabilizes the closed backdoor configuration. The transient, open backdoor configuration was modeled using the barbed-end conformation of F-actin, which exhibits a permanently open backdoor. C. Conformational equilibrium of the D-loop (pink) and its interactions with the upper long-pitch neighbor (yellow).

Cryo-EM studies of F-actin show that polymerization repositions Q137 and H161 closer to the γ-phosphate (Merino et al., 2018; Chou and Pollard, 2019; Oosterheert et al., 2022). Q137 moves approximately 1Å and H161 moves approximately 2.4 Å closer to the γ-phosphate, accompanied by a ~120° rotation. These movements allow a repositioning of W_{nuc} and a bridging water molecule (W_{bridge}) within the narrower nucleotide-binding pocket (Figure 2A, central panel). In F-actin, W_{nuc} is positioned within 3.6 Å of the γ-phosphate and remains hydrogen-bonded to Q137. W_{bridge} interacts with W_{nuc} and is further hydrogen-bonded to D154 and H161, forming a crucial hydrogen-bonding

 doi:10.20944/preprints202604.2036.v1

network responsible for activating W_{nuc} and transferring a proton, completing a geometry conducive to ATP hydrolysis (Oosterheert et al., 2022). These subtle rearrangements are enabled by subunit flattening and inter-subunit interactions, particularly along the long-pitch helical axis where the D-loop and the target-binding groove interact.

High-resolution cryo-EM structures reveal that coordinated water molecules and the divalent cation (Mg^{2+} or Ca^{2+}) play key-roles in stabilizing the active site (Oosterheert et al., 2022). Notably, Mg^{2+}-F-actin hydrolyzes ATP more rapidly than Ca^{2+}-F-actin, owing in part to differences in solvation geometry. In Mg^{2+}-actin, the metal ion is coordinated by the β-phosphate and four water molecules arranged for catalysis, while Ca^{2+}-F-actin displays a displaced solvation shell and less optimal geometry. These structural features explain why hydrolysis is tightly coupled to polymerization: only in the flattened, filament-bound conformation is the active site competent for catalysis.

2.2. Pi release and filament aging

Although ATP hydrolysis itself occurs rapidly, the release of the inorganic phosphate (Pi) product is delayed with a half-life is in the several minutes range. This delay results in a kinetically distinct ADP.Pi state that dominates in the "young" regions of filaments. The transition from ADP.Pi to ADP is structurally subtle but functionally critical for filament aging and disassembly.

Pi release occurs through a gated channel near the nucleotide-binding site, often referred to as the "backdoor" (Wriggers and Schulten, 1999). This conduit is sealed in both pre- and post-hydrolysis conformations under static conditions. Opening the backdoor requires a rearrangement involving a network of residues including R177, N111, H73, and G74, which collectively stabilize the closed state of the backdoor through a hydrogen bonding network (Oosterheert et al., 2023) that needs to be disrupted to open the backdoor (Figure 2B).

Molecular dynamics studies suggest that phosphate escape is stochastic and rare in the filament core, requiring transient disruption of the backdoor network (Wang et al., 2024; Oosterheert et al., 2023). This conformational fluctuation is not easily captured by cryo-EM, implying that Pi release involves short-lived intermediate states (Oosterheert et al., 2025; Oosterheert et al., 2023). The same backdoor is constitutively open at the filament's barbed end, explaining why phosphate release there is orders of magnitude faster (~2 s^{-1}) compared to the core (~0.006 s^{-1}). Thus, in the core subunits, backdoor opening is infrequent, structurally constrained, and represents the rate-limiting step in the aging process.

As actin filaments grow, they become progressively older with distance from the barbed end. This age gradient is marked by a shift in nucleotide composition from ATP- and ADP.Pi-bound subunits near the barbed end to ADP-bound subunits in the interior and near the pointed end. Structural studies suggest that this transition is not marked by a binary switch but rather by a gradual accumulation of local conformational changes (Dominguez, 2019; Merino et al., 2020). ADP-F-actin exhibits slightly increased subunit flexibility, particularly in the D-loop and C-terminal tail. These domains are more dynamic in aged (ADP-bound) filaments, providing potential recognition motifs for ABPs like cofilin (Chou et al., 2022; Oosterheert et al., 2022).

Furthermore, aging is associated with reduced filament stiffness. Experimental measurements indicate that ADP–Pi filaments have longer persistence lengths (~13.5 μm) than ADP filaments (~9 μm), reflecting differences in inter-subunit stability (Prochniewicz et al., 2005; Merino et al., 2020). These changes likely arise from alterations in the D-loop packing and C-terminal interactions that weaken longitudinal cohesion. The cumulative effect is that filament aging proceeds via a continuum of subtle conformational drift, allowing the cytoskeleton to encode temporal information via structure.

Despite remarkable progress, several key aspects of filament aging remain unclear. (1) Transient backdoor states: While cryo-EM provides snapshots of closed conformations, the intermediate required for Pi escape has not yet been directly observed. (2) Subunit cooperativity: Whether Pi release in one subunit influences neighboring subunits remains debated. Most models treat Pi release as stochastic and subunit-autonomous, but emerging simulations hint at possible allostery. (3)

 doi:10.20944/preprints202604.2036.v1

Quantitative conformational metrics: Although flattening is well characterized, finer conformational metrics (e.g., changes in torsional angle, hydration shell, or internal residue packing) are not consistently defined across the available structural studies. Future time-resolved cryo-EM or integrative approaches combining simulations and spectroscopy may help to bridge these gaps.

3. Nucleotide-Dependent Modulation of Actin Filament Properties

While the canonical transition from ATP to ADP through an ADP.Pi intermediate has long been associated with filament aging and ABP recognition, it also governs the structural, kinetic, and conformational states of the actin filament itself. These transitions influence the architecture of individual subunits and the cooperative behavior across the filament, the efficiency of polymerization, and the conformational ensembles available to the polymer. ATP-F-actin protomers polymerize more readily than their ADP-bound counterparts, a phenomenon first characterized through measurements of critical concentration and elongation kinetics (Pollard, 1986). ATP-F-actin exhibits a lower critical concentration at the barbed end (~0.1 μM) compared to ADP-F-actin (~2 μM), reflecting more favorable on-rates and more stable subunit incorporation (Pollard, 2016).

3.1. Nucleotide pocket, D-loop, and C-terminus

High-resolution cryo-EM data generally indicate that the overall conformation of F-actin changes minimally as a function of the bound nucleotide (Dominguez, 2019), but there are some subtle differences. In ATP-F-actin, the D-loop (residues 39–51) is predominantly in an open state (Figure 2C), which creates a hydrophobic cavity filled by the C-terminal residue F375 from the of an adjacent, long-pitch neighbor subunit, forming a hydrophobic network (Merino et al., 2018). The tight inter-subunit complementarity results in a structurally robust filament core.

In the ADP-Pi state the filament maintains many of the features of the ATP-bound conformation but with subtle changes in the nucleotide cleft and the C-terminus. The relative population of the D-loop closed state, which is primarily in the closed state that disrupts the hydrophobic interactions with F375, is increased after hydrolysis, but open-state D-loops are still present (Merino et al., 2018). The presence of inorganic phosphate (Pi) retains some of the inter-subunit cohesion, yet signs of weakening appear as a consequence of the D-loop changes and reduced order of the C-terminus.

In the ADP state, the D-loop is locked in the closed state with the open state not being observed. Additionally, the nucleotide cleft opens slightly, and the C-terminus adopts a helical conformation (Chou and Pollard, 2019; Merino et al., 2018). These changes correlate with decreased filament stability and stiffness, increased off-rate of subunits at the pointed end, and enhanced recognition by ABPs such as cofilin (Chou and Pollard, 2019).

3.2. Phosphate release backdoor and D-loop dynamics

The backdoor formed by the side-chains of residues R177 and N111, along with the backbones of methylated H73 and G74 (Figure 2B), remains predominantly closed in filaments but opens transiently, facilitating increased Pi escape and contributing to the aging process (Oosterheert et al., 2025; Oosterheert et al., 2023). The D-loop adopts a conformational equilibrium that shifts according to the nucleotide state of the actin protomers. These features suggest that the actin filament is not a uniformly composed polymer but rather a mosaic of subunits occupying different substates, particularly during the transition from ADP.Pi to ADP. Such variability enables graded regulation of filament behavior and provides a structural basis for allosteric modulation. MD simulations offer access to the filament's conformational ensemble.

Coarse-grained simulations and all-atom MD simulations showed that nucleotide identity also affects D-loop dynamics and modulates the strength of inter-subunit interactions (Chu and Voth, 2005). The simulations confirmed that D-loop mobility increases markedly in the ADP state, disrupting the cooperative hydrogen-bonding network along the long-pitch helix. A combination of enhanced sampling techniques with unbiased MD to map the energetics and pathway of phosphate

 doi:10.20944/preprints202604.2036.v1

release from filament subunits (Oosterheert et al., 2023; Wang et al., 2024) confirmed that phosphate escape requires transient backdoor opening and that opening probability is influenced by the conformational state of neighboring subunits. This supports a model of short-range cooperativity, in which conformational transitions at one subunit affect the energetics of adjacent protomers.

Together, these data reinforce the idea that nucleotide-dependent modulation is embedded in a network of inter-subunit mechanical coupling rather than strictly localized. These insights extend and complement the static cryo-EM data, suggesting a filament that dynamically responds to the distribution of nucleotide states across its length. LifeAct, a short actin-binding peptide that binds to F-actin's hydrophobic pocket (Belyy et al., 2020), has shown variable affinity depending on nucleotide state (Riedl et al., 2008; Belin et al., 2014), hinting at subtle structural differences in the target-binding groove (Kumari et al., 2020). These observations, though indirect, support the idea that nucleotide identity reshapes the filament surface in ways that affect protein interactions even in the absence of ABPs.

4. Mechanical Properties of Actin Filaments: Stiffness, Torsion, and Force Response

Actin filaments are semiflexible polymers that can bend and fluctuate while retaining structural integrity, giving rise to mechanical properties finely tuned to support wide range of cellular processes, including cell motility, mechanotransduction, endocytosis, and cytokinesis (De La Cruz and Gardel, 2015). In the cellular environment, actin filaments organize into networks through the function and coordination of a series of ABPs. These networks' ability to withstand and respond to mechanical forces depends not only on polymer length and network organization but also on intrinsic features of the filament core, including its stiffness, torsional rigidity, and dynamic structural adaptability. While crosslinking ABPs and accessory factors such as cofilin, myosin, and ARP2/3 complex modulate filament behavior at the network level, the mechanical characteristics of the bare filament core provide the structural basis for these higher-order functions (Blanchoin et al., 2014).

4.1. Bending stiffness

Actin filaments exhibit high axial stiffness, with a bending persistence length generally agreed upon to be around 10 μm in vitro under physiological ionic conditions (Pollard, 2016). This intrinsic stiffness arises from both intra-subunit rigidity, with inorganic phosphate rigidifying actin subunits, and tight inter-subunit packing along the filament. Cryo-EM reconstructions reveal that strong interfacial engagement, including new salt bridges at the nucleotide-binding cleft (von der Ecken et al., 2014) and the formation of a bridge between subunits by a magnesium ion at a specific cation-binding site in the presence of physiological Mg^{2+} and K^{+} (Xu et al., 2024), serves to limit thermal bending fluctuations and maintain filament straightness over micron scales (Bibeau et al., 2023).

Flexibility is significantly modulated by ionic strength, as actin filament mechanical properties depend on solution conditions, specifically monovalent and divalent cations (Kang et al., 2013). Binding of cations introduces additional hydrogen bonds across the protomers near a salt bridge, E167–K61, between SD1 and SD2 of the neighboring protomer, allosterically affecting the orientation and stability of the D-loop, and leading to an increase in stiffness (Xu et al., 2024). In the absence of ions at that site, filaments display a broader ensemble of conformations correlated with decrease in flexibility. This observation supports a structural continuum between rigid and flexible states.

The nucleotide state does contribute to filament stiffness (e.g., ADP.Pi–F-actin is stiffer than ADP–F-actin), but its effect is small compared to that of salt conditions and accessory proteins. For instance, accessory proteins like cofilin are known to render filaments more compliant in bending and twisting (Goode et al., 2023). Thus, intrinsic filament stiffness is more strongly governed by the physicochemical environment, bound ABPs, and subunit packing geometry than by the identity of the bound nucleotide.

 doi:10.20944/preprints202604.2036.v1

4.2. Torsional stiffness

High-resolution cryo-EM of bent filaments reveals a striking bend–twist coupling where filament axis curvature induced alternating overtwisting and undertwisting of filament strands (Reynolds et al., 2022). The structures show subtle variations in helical parameters that reflect how F-actin responds to mechanical forces, providing insight into its torsional flexibility. For instance, ADP-F-actin was found to be more deformable with greater twist deviations than ADP.Pi-F-actin for a given curvature. Cofilin binding also significantly alters filament twist, with abrupt changes occurring at boundaries between bare and cofilin-decorated segments (Huehn et al., 2020).

Bending and twisting of actin filaments are not independent. Actin filaments store elastic strain energy when twisted, and twisted filaments typically dissipate this torsional strain by supercoiling. However, pulling forces (tension) inhibit supercoil formation, which in turn causes twisted filaments to sever if the torsional strain cannot be dissipated (Bibeau et al., 2023). This indicates that under tension, the ability to relieve mechanical load through supercoiling is restricted, leading to retained torsional strain and potential fragmentation.

Actin filaments are semiflexible polymers that respond to mechanical forces through both elastic and plastic mechanisms. Elastic responses include stretching, bending, and twisting within a given conformational state, and are characterized by the storage of elastic strain energy. Plastic responses involve transitions to alternative structural states, such as supercoiling (plectoneme formation) and fragmentation (severing) (Bibeau et al., 2023). These responses arise from rearrangements in subunit packing and alterations in the inter-subunit hydrogen-bonding network. Filament twisting applied with magnetic tweezers causes filaments to supercoil into plectonemes, and pulling forces can prevent plectoneme formation and fragment filaments. Twist-extension response and thermally driven twist fluctuations suggest a torsional persistence length of approximately 10 μm, comparable to the bending persistence length (Bibeau et al., 2023). Twisting a filament bundle would require significantly more torque due to stiffness scaling.

4.3. Impact of post-translational modifications and sequence differences

Emerging evidence shows that specific post-translational modifications (PTMs) and chemical modifications influence actin filament mechanics by altering protomer structure and inter-subunit cohesion (Varland et al., 2019). For instance, oxidation of methionine 44 (Met44) within the D-loop of actin by Mical can lead to a less flexible and more hydrophilic sulfoxide, which in turn weakens hydrophobic actin–actin interactions and consequently results in filament disassembly (Grintsevich et al., 2017). This Mical-mediated oxidation has been linked to catastrophic disassembly of actin filaments. Similarly, phosphorylation of accessory proteins like cofilin (e.g., the phosphomimetic S3D-cofilin mutant) (Elam et al., 2017) can affect their binding to actin and severing activity; a single bound S3D-cofilin forms fewer contacts with actin and does not visibly affect the actin filament structure, in contrast to wild-type cofilin.

A comparison of mammalian (vertebrate) and yeast actin isoforms show that single amino acid substitutions can substantially shift filament conformational equilibria. Yeast actin filaments are more flexible and lack the salt-dependent stiffness observed in vertebrate actin (Kang et al., 2013). This difference can be attributed to the substitution of the glutamic acid at residue 167 (E167, involved in the E167-K61 salt bridge) in vertebrate actin by an alanine (A167) in yeast actin (Xu et al., 2024). Introducing an A167E mutation in yeast actin conferred salt-dependent stiffness similar to vertebrate actin. This underscores the principle that local sequence and chemical modifications (such as ion binding) tune mechanical properties through subtle changes in side-chain interactions at interfacial hotspots.

4.4. Impact of cofilin

Cofilin is a well-characterized severing protein that binds preferentially to ADP–actin filaments and undertwists the filament by approximately 4.3 degrees per subunit (Galkin et al., 2011). This

 doi:10.20944/preprints202604.2036.v1

changes the twist of F-actin and is known to increase the bending flexibility and torsional flexibility of actin filaments. These structural deformations also contribute to mechanical heterogeneity within the filament. Cryo-EM studies demonstrated that conformational changes in actin are limited to subunits in direct contact with cofilin (Huehn et al., 2018). Structural changes do not appear to propagate beyond these directly bound subunits and the filament twist changes abruptly at boundaries between bare and cofilin-decorated segments, without propagating into the bare actin. This indicates that the geometry of cofilin cluster boundaries is determined by local, nearest neighbor interactions, rather than long-range effects. Consequently, severing occurs preferentially at these mechanical boundaries where cofilin-decorated and undecorated segments meet, as local twist strain at these boundaries drives filament severing (Huehn et al., 2020). This localized stress, especially when combined with pulling forces generated by myosin motors, can dramatically accelerate filament fragmentation and turnover.

4.5. Modeling considerations

Actin filaments are often modeled as worm-like chains (WLCs), a common and effective framework for semiflexible polymers (Marantan and Mahadevan, 2018). In this model, the mechanical behavior is governed by the persistence length, which defines the length scale over which thermal fluctuations affect filament orientation. However, the classic WLC theory, which treats polymers as continuous, homogeneous, and isotropic elastic rods, does not fully capture all the complex mechanical behaviors observed in F-actin. For example, twist-bend coupling is a significant aspect of actin filament deformation (Reynolds et al., 2022). This coupling means that twisting a filament can induce bending, and vice versa, which is a more complex behavior than typically captured by a simple WLC model. Another example is the ability to switch between conformational substates. Actin filaments exhibit a structural landscape of co-existing conformations and can undergo structural transitions in response to mechanical load. This concept of discrete conformational changes and transitions is beyond the scope of a continuous elastic rod model, which primarily describes continuous elastic deformation within a given state.

More sophisticated monomer-based (Lyons et al., 2025) or agent-based (Banerjee et al., 2024) models are emerging that are more suitable to capture the nuanced, localized, and context-dependent mechanical behaviors arising from the complex molecular architecture of actin and its interactions with regulatory proteins.

The mechanical properties of actin filaments emerge from a balance of structural rigidity, conformational plasticity, and cooperative transitions. High-resolution reconstructions have clarified the role of inter-subunit packing and ion coordination in maintaining stiffness, while single-molecule experiments and simulations have shown how torsional and bending responses vary under load. Severing proteins such as cofilin reshape these properties by introducing structural heterogeneity that primes filaments for breakage. In summary, actin filament mechanics are not static but modulated by cellular context, chemical environment, and structural transitions. The actin core thus serves not only as a scaffold but also as a mechanically active element capable of sensing and responding to force, a property essential for its cellular function.

5. Barbed and Pointed End Dynamics: Regulation of Elongation and Disassembly

Actin filament dynamics are fundamentally polarized due to functionally distinct ends. Subunits associate and dissociate at markedly different rates at the two filament ends:. The "plus" (barbed) end supports faster monomer addition and growth, while the "minus" (pointed) end adds subunits more slowly and is more prone to disassembly. This polarity is fundamental to filament dynamics and underlies and underlies directional growth, treadmilling, and spatially controlled cytoskeletal remodeling (Pollard and Borisy, 2003). The structural basis of this asymmetry lies in distinct conformational states of the monomers residing at the barbed and pointed ends, shaped by local

 doi:10.20944/preprints202604.2036.v1

nucleotide content, inter-subunit interactions, and end-binding regulatory proteins (Courtemanche and Henty-Ridilla, 2024).

5.1. Barbed end structure and elongation

The barbed end is structurally adapted for rapid subunit addition (Pollard, 2016). High-resolution cryo-EM structures of undecorated vertebrate actin filaments reveal open backdoor conformations at the barbed terminus (Oosterheert et al., 2023). These open backdoors are characterized by the destabilization of the hydrogen bonding network involving the sidechains of R177 and N111, leading to the emergence of a cavity connecting the nucleotide-binding site to the filament exterior (Figure 2C). This structural arrangement facilitates rapid Pi release, making Pi release from barbed ends orders of magnitude faster than from core subunits. The ultimate subunit at the barbed end is largely in a flattened, F-actin-like conformation (Figure 3A) but has its W-loop (residues 165–172), in a position incompatible with a bound long-pitch neighbor (Figure 3D) and needs to rearrange. In particular, the side chain of Y169 has to undergo a substantial rotation to accommodate the D-loop of the incoming protomer. Additionally, the side chains of Y166 and E167 have to get into position to form and stabilize a salt bridge with K61 of the incoming subunit and to allow coordination of the stiffness cation (Xu et al., 2024).

The structural asymmetry between the terminal and penultimate subunits permits elongation while maintaining filament integrity (Carman et al., 2023). This region exhibits elevated conformational heterogeneity, consistent with rapid nucleotide exchange and subunit incorporation. Molecular dynamics simulations confirm the dynamic nature of this interface, for instance, by showing the mechanism of rapid Pi egress from the open backdoor at the barbed end (Oosterheert et al., 2023).

In the cellular environment, actin does not spontaneously polymerize; it is maintained in its monomeric (G actin) form through interactions with proteins such as profilin and thymosin. Its nucleation is tightly regulated by a set of actin nucleators; the Arp2/3 complex and formins. Formins are homodimeric proteins that function both as nucleators, initiating the formation of new actin filaments, and as processive elongation factors. They remain attached to the growing end of filaments, facilitating the incorporation of profilin bound actin monomers and significantly accelerating filament growth (Pollard, 2016). The structural basis of formin-mediated elongation was elucidated by cryo-EM structures of the FH2 domains of slow-, intermediate-, and fast-stepping formins (Cdc12, INF2, and mDia1) bound to actin filament barbed ends, including a complex with profilin-actin (Oosterheert et al., 2024). Previous models proposed that formins operate by rapidly alternating between "closed" and "open" states. Instead, formins appear to bind in a common asymmetric conformation to the native actin barbed end, and do not majorly alter the helical arrangement or induce large conformational changes in the terminal actin subunits (Oosterheert et al., 2024).

Instead, the formin–actin interface is characterized by an asymmetric ring-like structure where one FH2 hemidimer (the trailing FH2) is stably bound, while the other (the leading FH2) is loosely associated and available to capture a new subunit (Figure 3E). The key step in elongation involves the incoming actin subunit sterically displacing the trailing FH2 domain, which then undocks and steps forward, allowing the new subunit to "lock" into canonical filament contacts (Oosterheert et al., 2024). This coordinated process is termed the formin movement is directly coupled with actin subunit addition. Gating, in this context, refers to the extent that a formin sterically hinders the addition of a new subunit, influencing the rates of this transition.

 doi:10.20944/preprints202604.2036.v1

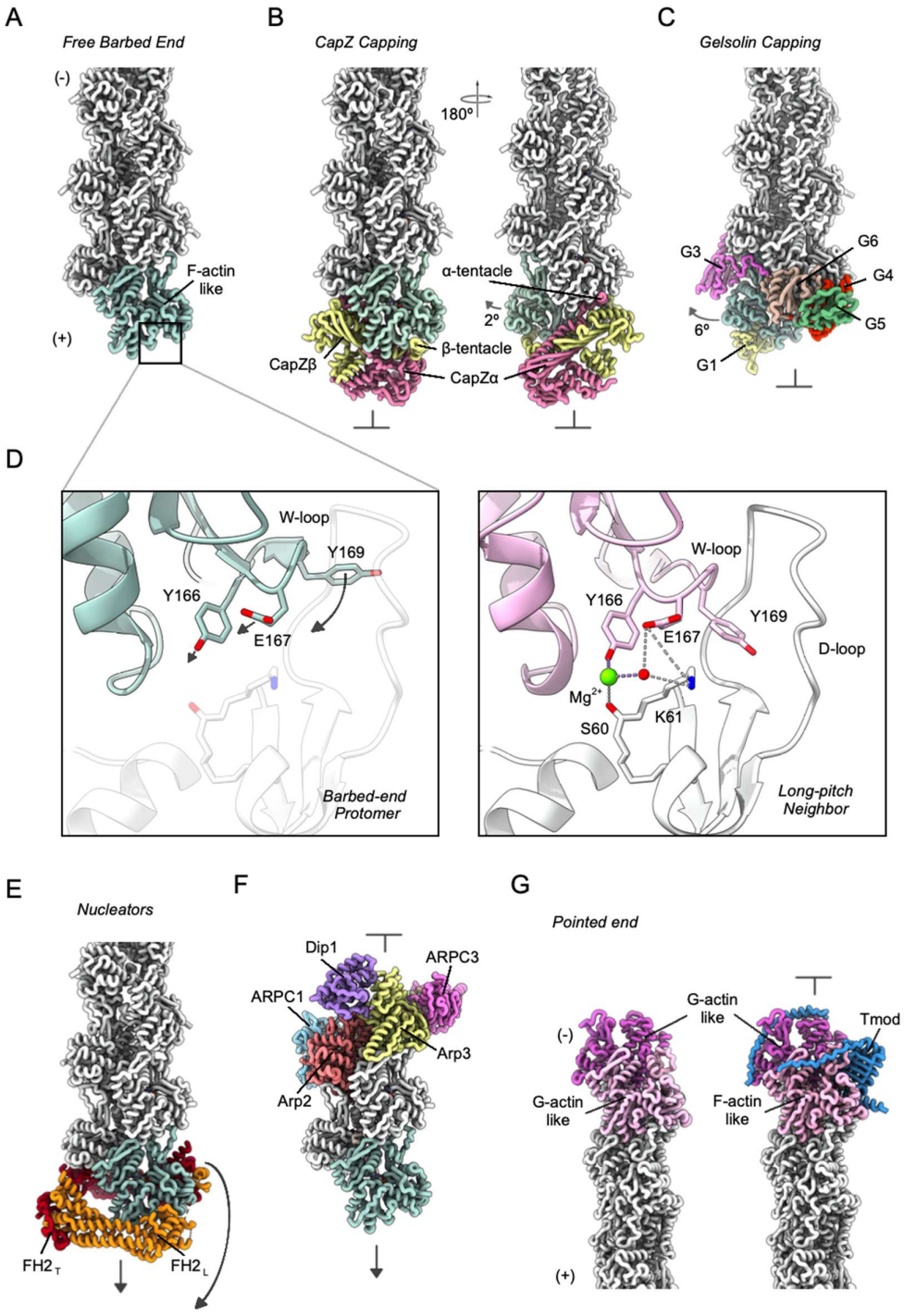

Figure 3. ***Barbed and pointed ends of F-actin.*** A. Structure of the free barbed end of F-actin. The pointed (-) and barbed (+) end are indicated. The terminal actin protomer (light blue) adopts an F-actin like, flattened conformation. The boxed region corresponds to the detail shown in (D). B. Structure of the CapZ-capped barbed end. Two views related by a 180º rotation are shown. CapZα and CapZβ are colored in pink and yellow, respectively. The 2º rotation of the terminal protomer (light blue) relative to the filament axis is indicated by an arrow. C. Structure of the gelsolin-capped barbed end. Gelsolin domains G1, and G3-G6 are indicated; G2 is bound adjacent to G3 but is not visible in this view. The 6º rotation of the terminal protomer (light blue) relative to the filament axis is indicated by an arrow. D. Structural differences between the terminal protomer and a core protomer in F-actin. The W-loop is shifted and requires rearrangement to accommodate a long-pitch neighbor (right panel). Sidechain movements are indicated by arrows. In core protomers, Y166 directly coordinates the

 doi:10.20944/preprints202604.2036.v1

stiffness Mg^{2+} cation, while E167 stabilizes a coordinating water (red sphere) through salt bridge formation with K61 of the long-pitch neighbor. E. Barbed-end nucleation by formins. The trailing FH2 hemidimer ($FH2_T$, red) is displaced by the incoming actin monomer and becomes the new leading FH2 hemidimer (grey arrow). The leading FH2 hemidimer ($FH2_L$, orange) subsequently transitions into the new $FH2_T$. F. Barbed-end nucleation (and pointed-end capping) by Dip1-activated Arp2/3 complex. Arp2 (orange) and Arp3 (yellow) form a barbed-end template for filament growth. G. Structures of the free pointed end (left) and tropomodulin-capped pointed end (Tmod, blue), In both, the terminal actin protomer (pink) remains in a G-actin like conformation. At the free pointed end, the penultimate protomer (light-pink) is also a G-actin-like conformation, whereas in the Tmod-capped end it is converted to an F-actin conformation.

In cells, G actin is held in a readily exchangeable state through its interaction with profilin, which serves as a key carrier of actin monomers to sites of filament growth. Profilin binds to the barbed-end target-binding cleft of G-actin (Dominguez, 2004). For elongation to proceed, profilin must be released from actin to allow its incorporation into the filament. Structural data from the actin-formin-profilin complex show that profilin's rapid release from actin is a consequence of the G- to F-actin transition that occurs upon subunit incorporation (Oosterheert et al., 2025). When profilin-bound G-actin incorporates into the filament and transitions to its flattened F-actin conformation, it causes a significant separation (approximately 7 Å) between actinformins, through steric competition with their FH2 domain, actively displace profilin from the barbed end (Oosterheert et al., 2024). This mechanism explains why formins accelerate profilin release from the F-actin barbed end, as their FH1 domains efficiently recruit profilin–G-actin, enhancing the likelihood of G-actin encountering the barbed end and thus driving faster filament growth.

5.2. Barbed-end capping

Capping proteins, such as CapZ (also known as capping protein or CP), are a heterodimer of structurally similar alpha and beta subunits that bind tightly to actin filament barbed ends, effectively blocking subunit addition and loss. This prevents further monomer addition and terminates filament elongation and disassembly at this end (Pollard, 2016). The molecular basis of CapZ interaction with the barbed end was revealed by a high-resolution cryo-EM structure of the CapZ-capped barbed end (Carman et al., 2023). CapZ adopts a mushroom-like shape where its head binds the barbed end. Both the CapZ alpha and beta subunits interact with the terminal and penultimate actin subunits. The α-tentacle (CapZα residues R260-A286) and β-tentacle (CapZβ residues H209-L243) project out to engage the hydrophobic binding clefts of these barbed-end subunits (Figure 3B).

CapZ is described as constitutively active, meaning it binds F-actin barbed end without requiring active signaling (Pollard, 2016). It recognizes the structural features of the barbed terminus itself (Carman et al., 2023). CapZ is essential for processes like maintaining the actin monomer pool and limiting the number of barbed ends available for growth during protrusion. In stark contrast to formins, which promote processive barbed-end growth, capping proteins like CapZ impose a static cap (Pollard, 2016). This emphasizes the structural versatility of the barbed end as both a site of dynamic growth and static arrest. Formins and CapZ can coexist at the barbed end in vitro, but simply overlaying their bound structures creates prominent steric clashes, suggesting that extensive rearrangements are needed for such a "decision complex" to form (Oosterheert et al., 2025).

Structural studies indicate that the terminal and penultimate actin subunits at the barbed end already adopt a flattened F-actin conformation prior to CapZ binding (Oosterheert et al., 2023). Upon binding, CapZ induces a splaying of the short-pitch pair formed by these two terminal subunits by approximately 1.5 Å, resulting from a ~2° rotation of the ultimate subunit away from the filament's longitudinal axis (Carman et al., 2023). CapZ itself undergoes major structural changes upon binding, adopting a flatter conformation and bending by ~15° from its filament-unbound state.

Gelsolin family proteins primarily function as severing proteins (Barrie et al., 2025). Gelsolin, which comprises of six domains denoted G1-G6, severs actin filaments by binding its G1, G2, and G4 domains in the barbed-end groove, then remains firmly associated with the newly created barbed

 doi:10.20944/preprints202604.2036.v1

end (Figure 3C). This stable association is key to its capping mechanism, as it effectively blocks both subunit addition and loss at the barbed end, inhibiting monomer exchange. Specifically, domains G1 and G4 occupy the hydrophobic clefts of the two terminal actin subunits, preventing incoming monomers from binding to the barbed end. The ultimate subunit undergoes a rotation of approximately 6° away from the main F-actin axis, displacing residues at the barbed end by up to 5.5 Å and thought to be essential for the severing activity of gelsolin (Barrie et al., 2025).

5.3. Pointed end structure and dynamics

The pointed end of an actin filament displays distinct structural features that contribute to its slower dynamics for both subunit addition and dissociation, a long-standing observation in actin polymerization kinetics (Pollard, 2016). High-resolution cryo-EM structures of the undecorated F-actin pointed end have consistently revealed that the two terminal subunits at the undecorated pointed end adopt a twisted, G-actin-like conformation (Boiero Sanders et al., 2024; Carman et al., 2023) (Figure 3G). This is in stark contrast to the barbed end, where all subunits adopt a flattened, F-actin-like conformation.

The structural arrangement at the pointed end has several implications for its dynamics (Boiero Sanders et al., 2024). The G-actin-like conformation of the terminal subunits at the pointed end differs significantly from the flattened F-actin conformation of internal subunits and at the barbed end. In particular, the D-loop, which forms a major longitudinal contact in the filament core (Das et al., 2020), is disordered and flexible in these terminal pointed-end subunits. This means that the D-loops of the two exposed subunits at the pointed end have no lateral or longitudinal interactions (Chou and Pollard, 2019), leading to a lack of stabilizing inter-subunit contacts that would otherwise favor polymerization or resist dissociation.

When a new monomer attempts to add to the pointed end, it can remain in a G-actin-like state. However, the penultimate subunit is required to flatten to accommodate the incoming monomer (Boiero Sanders et al., 2024). This flattening is restrained by its existing interactions with four other actin subunits within the filament, creating a kinetic barrier that impedes monomer addition. This is conceptually analogous to the unfavorable initial steps of actin nucleation (i.e. G-actin to G-actin interactions) (Carman et al., 2023). Similarly, for dissociation to occur, the internal subunit to become the penultimate subunit would need to undergo a conformational change (F- to G-actin unflattening). However, this subunit is conformationally more restricted due to its multiple inter-subunit contacts compared to a subunit at the barbed end, which can convert relatively freely from an F-actin to a G-actin configuration for dissociation (Boiero Sanders et al., 2024). This explains why dissociation rates at the pointed end are lower compared to those at the barbed end.

Despite the comparatively low dissociation rates, the pointed end plays a principal role in filament disassembly within the cell. This is achieved by depolymerization factors such as Cyclase-Associated Protein (CAP), which promote rapid pointed-end depolymerization, most likely by weakening the packing between the ultimate and the penultimate actin subunits (Oosterheert et al., 2025). Another important regulator of pointed-end dynamics is Tropomodulin (Tmod), which is exclusively a pointed-end capping protein (Fischer and Fowler, 2003). Tmod wraps around the three terminal subunits at the pointed end, effectively blocking subunit addition and loss (Carman et al., 2023). This extensive interaction stabilizes the pointed-end arrangement, in part by bridging these terminal subunits and actively forcing the penultimate actin subunit into an F-actin-like conformation (Figure 3F). This conformational change is significant, as the penultimate subunit's flattening is otherwise a kinetic barrier for new monomer addition at the pointed end (Oosterheert et al., 2025).

5.4. Barbed-end nucleation by Arp2/3 complex

The Arp2/3 complex plays a pivotal role in the dynamic regulation of actin by nucleating new actin filaments from the sides of existing "mother" filaments, thereby creating a branched network (Blanchoin et al., 2000). This process is essential for various cellular movements and functions, as the newly formed (Pollard et al., 2000). In its activated state, the Arp2/3 complex undergoes a

 doi:10.20944/preprints202604.2036.v1

conformational change, where its two actin-related protein subunits, Arp2 and Arp3, move closer together, positioning them into a short-pitch arrangement that effectively mimics an F-actin dimer (Volkmann et al., 2001). This F-actin-like conformation then serves as a platform for the first incoming actin monomers, thereby templating the initial steps of daughter filament barbed-end elongation.

High-resolution cryo-EM structures of the Arp2/3 complex branch junction reveal that the mother filament in contact with the Arp2/3 complex is slightly bent and twisted (Chavali et al., 2024), consistent with its preference for binding to curved actin filaments (Risca et al., 2012). This slight local deformation of the mother filament, which can arise from intrinsic twist-bend coupling properties of actin or thermal motions, facilitates stable binding and nucleation by the Arp2/3 complex.

Mimicking the G-actin to F-actin transformation both Arp2 and Arp3 subunits in the Arp2/3 complex transition from a "twisted" (G-actin-like) to a "flattened" (F-actin-like) conformation (Ding et al., 2022; Chou et al., 2022). This flattening is critical for templating the daughter filament, as it widens the barbed end groove of the Arps, allowing the D-loops of the first two daughter actin subunits to properly insert and form intrastrand filament contacts between them (Ding et al., 2022). The flattening of Arp3 increases its contacts with the mother filament, suggesting that mother filament binding together with binding of nucleation-promoting factors (NPFs) stimulates this conformational change in Arp3. The free barbed end of the daughter filament elongates rapidly, further enhanced by co-factors such as formins (Pollard, 2016).

Beyond its well-established function in nucleating branched actin networks, the Arp2/3 complex also exhibits a distinct, less prominent role as a pointed-end capping protein (Volkmann et al., 2014). This capping activity can occur independently of NPFs or actin monomers, directly binding to the pointed end of pre-formed actin filaments. The NPF Dip1 leads to a similar arrangement by uniquely activating the Arp2/3 complex to nucleate linear actin filaments without requiring a preformed mother filament (Wagner et al., 2013). This distinguishes it from other NPFs, which need an existing filament for branching. Similar to the mechanism in branch formation, Dip1 facilitates activation by positioning Arp2 and Arp3 into a short-pitch arrangement, mimicking an F-actin dimer that templates new filament assembly (Figure 3F). Unlike Arp2/3 in branches (Shaaban et al., 2020), Dip1-activated Arp2/3 remains stably associated with the pointed end of the nucleated filament, likely due to a lack of rapid ATP hydrolysis on Arp2/3 (Ding et al., 2022).

The dynamics of actin filament ends are shaped by a balance of structural asymmetry, nucleotide state, and end-binding regulatory proteins. The barbed end is structurally equipped for fast growth, modulated by processive formin gating or capping termination. In contrast, the pointed end is structurally disadvantaged for elongation but optimized for controlled disassembly. High-resolution structures have revealed key differences in inter-subunit interactions, conformational flexibility, and nucleotide release behavior at the ends, defining a structural logic for polarized actin dynamics. Essential for cell motility and membrane remodeling, branched actin networks are generated by the Arp2/3 complex, which undergoes a conformational shift that mimics an actin filament barbed end, enabling stable binding to mother filaments and templating the growth of daughter filaments.

6. Actin-Binding Proteins: Mechanisms of Filament Interaction and Modulation

Actin-binding proteins (ABPs) regulate actin filament function by binding to the filament and altering the conformation, surface chemistry, and mechanical properties of its subunits (Pollard, 2016). These interactions can be highly localized, affecting only the binding site, or cooperative, propagating conformational changes to neighboring protomers. Most ABPs interact with the target-binding cleft (also known as the hydrophobic cleft), located between subdomains 1 and 3 of the actin protomer. This cleft serves as a key interaction site, where ABPs often insert an amphiphilic α-helix to anchor themselves to actin (Dominguez and Holmes, 2011). ABPs fulfill diverse functions, including nucleating new filaments, promoting elongation, capping filament ends, severing filaments, cross-linking filaments, and binding G-actin monomers (Pollard, 2016). This subchapter focuses on the structural impact of ABPs on actin filaments, specifically on ABP-induced alterations to filament architecture, stability, and dynamics.

 doi:10.20944/preprints202604.2036.v1

6.1. Severing proteins

Cofilin and gelsolin are two major ABP families that regulate filament dynamics through severing. While both disassemble actin filaments, they differ markedly in size, regulation, binding specificity, structural impact, and cellular roles (Pollard, 2016). Cofilin (~15 kDa) is primarily regulated by phosphorylation of Ser3, which blocks its actin binding and severing. Cofilin binds cooperatively along the filament side, inducing significant local structural rearrangements in the actin subunits. Cryo-EM studies reveal that cofilin binding is associated with under-twisting of actin subunits and a dramatic ~30° rotation of subdomains 1 and 2 (Huehn et al., 2020). These changes displace the actin D-loop and weaken longitudinal subunit contacts, destabilizing the filament. Severing occurs preferentially at the boundaries between cofilin-decorated and bare actin segments (Huehn et al., 2018). Cofilin has higher affinity for ADP-actin than ATP-actin and primarily severs F-actin in the ADP state (Oosterheert et al., 2022).

Gelsolin family proteins are large, multi-domain proteins activated by calcium binding, which releases them from an autoinhibited state. Cryo-EM data show that domains G1 and G4 insert helices into the hydrophobic clefts of the two actin subunits along the long-pitch helix of the filament with full-length gelsolin (G1-G6) wrapping around the barbed end (Barrie et al., 2025). Initial binding of G2 and G3 rotates an adjacent subunit away from the filament axis by up to about 6 Å (Figure 3C), disrupting D-loop contacts and enabling Gelsolin G1 to insert into the exposed target-binding cleft. This acts as a wedge that strains and severs the filament. Following severing, gelsolin remains bound to the barbed end, capping it and blocking subunit exchange, a direct consequence of its severing mechanism (Barrie et al., 2025).

6.2. Contractile machinery

The cell's contractile machinery relies on large families of actin-binding proteins, most prominently myosins (Robert-Paganin et al., 2020) and tropomyosins (Gunning et al., 2015a). Myosins bind actin filaments to generate force and movement and tropomyosins stabilize filaments and regulate myosin access, together enabling coordinated contraction and cytoskeletal organization. Myosin binding consistently induces structural and dynamic changes within F-actin. A common effect observed across different myosins is the modulation of the actin D-loop conformation (Gong et al., 2022; Pospich et al., 2021). For instance, the D-loop coexists in the open and closed states when rigor Myosin-15 is bound. However, ADP-bound Myosin-15 locks the D-loop constitutively in the closed conformation, restricting its flexibility and overriding nucleotide-state-dependent rearrangements (Gong et al., 2022). Similarly, Myosin-5 binding overrules actin nucleotide-state-dependent D-loop rearrangements, constitutively locking it in a closed conformation (Pospich et al., 2021). This common influence on the D-loop suggests a shared mechanism by which strongly-bound myosins can regulate actin polymerization and nucleation efficiency.

Beyond localized D-loop modulation, myosin binding can induce broader architectural changes, such as a global compression of the F-actin filament along its longitudinal axis by Myosin-15 (Gong et al., 2022), and an increased ordering of the D-loop region by Myosin-5 (Klebl et al., 2025). Different myosins exhibit unique kinetic and force-sensing properties and show considerable heterogeneity in structure and statistical coupling between their active site and structural domains (Pospich et al., 2021). However, the fundamental principle of myosin-induced structural and dynamic modulation of F-actin is broadly conserved across the superfamily. A significant commonality among myosin motors, despite their structural divergence, is their interaction with a conserved core interface on F-actin (Robert-Paganin et al., 2021). This core interface primarily involves the target-binding cleft on F-actin, providing a fundamental anchoring site for the motor on the actin filament. This implies a common principle of interaction despite local variations in myosin sequence.

The coiled-coil protein tropomyosin binds continuously along each of the two long-pitch helices of the actin filament. Its primary roles are to stabilize filaments and regulate interactions with other ABPs by modulating its azimuthal position on the filament (Gunning et al., 2015a). The regulatory troponin complex binds to actin filaments and triggers displacements of tropomyosin in in a calcium

 doi:10.20944/preprints202604.2036.v1

dependent manner (Risi et al., 2024). Cryo-EM studies of the F-actin–tropomyosin complexes show that the helical parameters of the F-actin are preserved upon tropomyosin binding, with minimal structural changes to individual actin subunits (von der Ecken et al., 2014). This suggests that tropomyosin functions not by altering the subunit conformation, but by forming extensive intra- and intermolecular contacts such as salt bridges and hydrophobic interactions with F-actin.

6.3. Crosslinking proteins

A large family of ABPs, coined crosslinkers, significantly influence the structure and dynamics of F-actin in vivo, exhibiting common mechanisms despite their diverse functions (Tseng et al., 2005). A fundamental commonality in their interaction with F-actin involves engagement with the target-binding cleft (Mei et al., 2022; Kumari et al., 2020; Iwamoto et al., 2018; Gong et al., 2025) that also provides the core interface for myosin (Robert-Paganin et al., 2021). Crosslinkers can induce broader structural and dynamic changes, often leveraging their own structural plasticity to adapt to F-actin

Filamin A, for example, engages F-actin through multiple actin-binding sites in the target-binding groove, with one of its two calponin-homology (CH) domains undergoing a reorientation to avoid steric clashes with F-actin and expose essential actin-binding residues (Iwamoto et al., 2018). This necessary mobility in the CH domain suggests that many conformations are compatible with actin binding. T-plastin, a crosslinkers also containing two CH domains (CH2) binds the target-binding cleft on F-actin and display substantial structural plasticity with significant rearrangements of its CH domains (Mei et al., 2022). Utrophin and spectrin, two CH2-domain-containing proteins that link actin to the plasma membrane, display similar behavior (Kumari et al., 2020; Li et al., 2023), supporting the existence of a shared mechanism underlying the binding of CH2-domain-containing ABPs.

Fascin, which cross-links F-actin into hexagonal bundles in structures like filopodia, does not contain CH domains but exhibits asymmetric F-actin binding and considerable structural plasticity that allows it to bridge varied interfilament orientations and accommodate mismatches between F-actin's helical symmetry and bundle packing (Gong et al., 2025). All four crosslinkers are reported not to substantially alter F-actin (Mei et al., 2022; Kumari et al., 2020; Iwamoto et al., 2018; Gong et al., 2025), suggesting that they primarily organize larger-scale F-actin architectures without deforming the filaments themselves.

6.4. Mechanotransduction proteins

The effect of force-sensitive ABPs like αE-catenin and vinculin on F-actin share many features with the crosslinker ABPs previously discussed. Cryo-EM studies reveal that both αE-catenin and vinculin binding cause minimal overall rearrangements to the F-actin filament, with its helical parameters remaining practically identical to bare F-actin (Mei et al., 2022; Xu et al., 2020). The most significant and localized effect on F-actin structure is observed in the D-loop conformation. αE-catenin maintains the D-loop in a closed conformation, similar to that seen in bare ADP-bound F-actin (Xu et al., 2020). While this overall state is maintained, key residues, particularly M47, undergo a significant displacement relative to bare ADP-actin. This suggests that αE-catenin (Mei et al., 2022; Xu et al., 2020). Furthermore, akin to the crosslinking ABPs, the actin-binding domains of both aE-catenin and vinculin exhibit substantial structural plasticity upon F-actin engagement. This involves conformational remodeling, such as N-terminal order-to-disorder transitions, and rearrangements in their helical bundles and C-terminal extensions, all necessary for binding and avoiding steric clashes.

This pattern of interaction extends to talin, a critical force-sensing scaffold within focal adhesions (Critchley, 2009). Talin possesses three actin-binding sites (ABS1, ABS2, and ABS3). High-resolution structural analysis of an F-actin-ABS3 complex shows that ABS3 binds by spanning two actin monomers along the filament axis (Biertümpfel et al., 2025). Stable engagement of ABS3 to F-actin is contingent upon dimerization through the DD domain. The R13 rod subdomain of one ABS3 and the dimerized DD domains each engage a distinct actin monomer, the R13 rod subdomain of the second protomer does not appear to bind to F-actin and is not visible in the structure. Similar to vinculin and

 doi:10.20944/preprints202604.2036.v1

αE-catenin, the talin R13 helical bundle undergoes significant distortions upon binding to F-actin, causing the release of its N-terminal helix, a phenomenon also observed in the other two tension-sensing proteins (Mei et al., 2020; Xu et al., 2020), highlighting a possible common mechanism for actin-based mechanosensitive actions. The DD binding interface of the bound ABS3 on F-actin shows a significant overlap with helices in vinculin and αE-catenin, indicating shared binding sites (Biertümpfel et al., 2025). Furthermore, αE-catenin, vinculin, and talin ABS3 have all been shown to exhibit force-induced catch-bond formation, where their binding affinities to F-actin increase in response to force (Huang et al., 2017; Buckley et al., 2014; Owen et al., 2022). Importantly, despite the extensive interactions, the binding of talin ABS3 to F-actin did not result in any observed movement of the D-loop or major changes to the F-actin structure itself (Biertümpfel et al., 2025). This observation reinforces the consistent finding that these force-sensitive actin-binding proteins achieve their mechanosensory roles and robust F-actin engagement with minimal large-scale structural perturbation to the actin filament itself.

6.5. Fluorescence probes

Numerous actin-binding proteins (ABPs) have been developed as fluorescent probes to visualize F-actin networks in live eukaryotic cells using fluorescence microscopy. Cryo-EM studies have provided detailed structural insights into two widely used probes, LifeAct and F-tractin (Belyy et al., 2020; Shatskiy et al., 2025). Both are amphipathic helices that bind overlapping interfaces within the hydrophobic region of the target-binding cleft, formed by subdomains 1 and 3 of one actin subunit and the D-loop of the adjacent subunit in the same filament strand. Interestingly, the small molecule fluorescence probe pyrene, commonly used for in-vitro polymerization assays, binds in an overlapping location as well (Chou and Pollard, 2020). The minimal structural impact of LifeAct and F-tractin on F-actin makes them valuable markers for visualizing filaments in diverse cellular contexts (Belin et al., 2014). However, because their binding sites overlaps with that of many other ABPs, potentially altering cell morphology (F-tractin) in some cases, show probe-specific biases. Lifeact favors lamellipodial networks and exclude lamellar and filopodial (Belin et al., 2014).

6.6. Toxins

Phalloidin and jasplakinolide (JASP) are widely utilized toxins that stabilize actin filaments and are also commonly employed as fluorescent labels in microscopy (Baltes et al., 2022). These small molecules bind to overlapping sites within the actin filament structure within the inter-strand groove, typically interacting with three adjacent actin protomers (Merino et al., 2018; Pospich et al., 2017). JASP consistently locks vertebrate F-actin into an open D-loop conformation, mimicking the ADP-Pi state independent of the actual nucleotide state, and, if present, strongly inhibits the release of Pi from the nucleotide-binding pocket of F-actin (Oosterheert et al., 2023; Merino et al., 2018).

Phalloidin's effect on the D-loop conformation depends on the timing of its addition: if added immediately before polymerization, it stabilizes the open D-loop state and reduces Pi release, similar to JASP. However, if added to ADP-F-actin, the D-loop remains in the closed state (Pospich et al., 2020). In any case, both toxins effectively keep the phosphate release backdoor closed (Oosterheert et al., 2023). Additionally, Phalloidin can bind to an ultimate site at the pointed end, bridging and flattening the two terminal subunits (Boiero Sanders et al., 2024). JASP is generally reported to stabilize F-actin more effectively than phalloidin, exhibiting a slightly stronger stiffening effect as evidenced by its greater increase in the persistence length of actin filaments (Pospich et al., 2020).

Beyond these toxins, the Salmonella effector SipA also functions as a potent F-actin stabilizer. Its C-terminal fragment (SipAC) binds to the same inter-strand groove as phalloidin and JASP and SipA binding exerts a similar stiffening effect (Niedzialkowska et al., 2024). Similar to the toxins, SipAC stabilizes the phosphate release backdoor in a closed conformation. In contrast to the toxins, however it exclusively binds to and stabilizes ADP-Pi actin (Yuan et al., 2023). The shared inter-strand binding mode of the two toxins and SipA underscores a common principle of F-actin stabilization by external molecules.

 doi:10.20944/preprints202604.2036.v1

ABPs constitute a highly diverse set of proteins that modulate filament architecture, stability, and dynamics through distinct structural mechanisms. Despite their varied functions, ranging from severing (for example cofilin and gelsolin) and stabilization (for example tropomyosin, toxins, SipA) to crosslinking, force transduction, and motor activity (for example myosins), many converge on a common interaction hotspot that includes, the target-binding cleft, the neighboring D-loop, and a distinct patch around residue 96 (Figure 4), using adaptable structural domains to anchor to actin without altering its helical parameters. In many cases, binding to these patches is complemented by interactions with additional specific regions on F-actin, which enhance binding specificity and can influence cellular function, cytoskeletal assembly, and morphology, showing how both the primary anchoring site and secondary interactions shape the outcome of ABP actin regulation (Figure 4).

7. Actin Sequence Variations: Isoforms, Mutations, and Evolutionary Divergence

Actin is one of the most conserved and essential proteins in eukaryotes, yet it exhibits a spectrum of isoforms, functional specializations, and disease-linked mutations. Vertebrates, including humans, express at least six distinct actin isoforms: α-skeletal, α-cardiac, α-smooth, enteric γ-smooth muscle, β-cytoplasmic, and γ-cytoplasmic (Pollard, 2016). These isoforms are essential for the functional organization of the eukaryotic cytoplasm, playing specific and non-redundant roles in various cellular functions, including muscle contraction, cell migration, and cell division Blanchoin et al., 2014 #69460}. Mutations or aberrant expression of these actin isoforms have been linked to a range of human diseases, such as cardiomyopathies, developmental disabilities, and cancers (Parker et al., 2020).

7.1. Actin isoforms

Despite their diverse functions, these actin isoforms are remarkably conserved at the sequence level, sharing high identity (93–99%) (Perrin and Ervasti, 2010), and high resolution cryo-EM studies confirm that filamentous actin isoforms maintain their characteristic helical parameters and overall structure (Heissler and Chinthalapudi, 2025). The breadth of these functional capabilities is made possible by the tightly coordinated regulation of actin, ranging from isoform expression and chaperone assisted G-actin folding, to the dynamic equilibrium between G-actin and F-actin, and the organization of actin supramolecular networks, all under the control of a large and diverse set of actin binding proteins (ABPs) (Pollard, 2016). These ABPs are remarkably sensitive to sequence variations and can differentially tune their interactions based on the small sequence variations among actin isoforms. For example, F-actin's nuanced interactions with myosin motors and other ABPs are enabled by subtle differences primarily attributed to amino acid substitutions in SD1, SD3, and SD4 (Arora et al., 2023). Interestingly, no substitutions are found in SD2 between vertebrate isoforms, suggesting strong selective pressure to maintain the critical structural role of SD2 (Heissler and Chinthalapudi, 2025).

 doi:10.20944/preprints202604.2036.v1

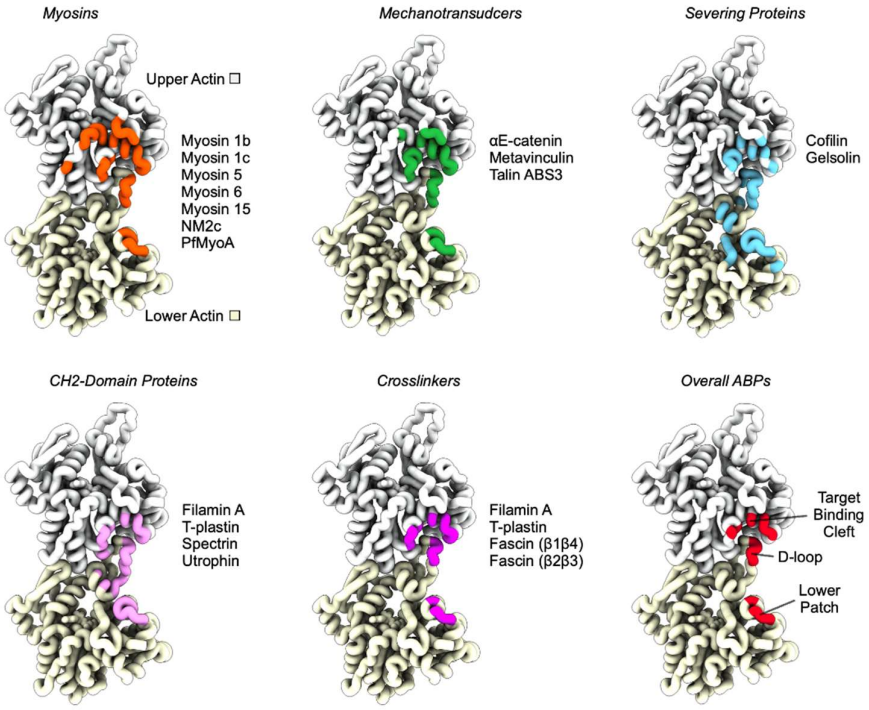

Figure 4. Common footprints of ABPs on F-actin compiled from high-resolution structures. Two long-pitch actin protomers (Lower and Upper Actin) are shown. The ABPs considered in each panel are listed to the right, with residues highlighted that are contacted by all ABPs listed. Three common patches contacted by all ABPs are indicated in red (lower right panel): (i) residues in the target-binding cleft (residues 143,146, 345, and 348-350), (ii) residues in the D-loop (residues 45-48) and (iii) residues on top of SD1 of the lower actin, centered around residue 96 (Lower Patch, residues 92, 96 and 97).

Vertebrate actin isoforms show the largest divergence at the acidic N-terminus within SD1 (Heissler and Chinthalapudi, 2025). For example, the N-termini of mature β-actin (DDD) and γ-actin (EEE) have different pKa values, leading to a higher negative electron charge density in β-actin compared to γ-actin, which is further increased by N-terminal acetylation in both isoforms (Arora et al., 2023). Cryo-EM reconstructions have resolved the N-termini of various human actin isoforms (Figure 5) , revealing isoform-specific structural arrangements that contribute to distinct binding interfaces (Arora et al., 2023). The N-terminus is prominently exposed on the filament surface, and its processing or modifications can locally alter the filament charge density, influencing interactions with ABPs and myosin motors.

Post-translational Modifications (PTMs), particularly N-terminal acetylation and H72/H73 methylation, are extensively conserved in vertebrate actins and are known to directly affect actin biochemistry and fine-tune cytoskeletal dynamics (Terman and Kashina, 2013). N-terminal acetylation, although historically challenging to resolve structurally using tissue-purified actins (Rebowski et al., 2020), has been resolved in recombinant β- and γ-F-actin structures (Arora et al., 2023). This modification can increase the elongation and depolymerization rates of mixed β-actin/γ-actin filaments and also boosts intrinsic and Arp2/3-mediated filament nucleation for β-actin, suggesting that non-acetylated actin is more stable (Drazic et al., 2018). Methylation of H72/H73, located in the nucleotide sensor loop in SD1, has a stabilizing effect on actin filaments by promoting polymerization (Guo et al., 2019). The high resolution of recent cryo-EM structures of human F-actin (2.6 – 2.9 Å) has allowed for the resolution of these key PTMs in the filament context (Arora et al., 2023).

The filament core exhibits high conservation, but subtle variations in side-chain packing occur at longitudinal and transverse inter-protomer interfaces. For instance, the transverse interface has

 doi:10.20944/preprints202604.2036.v1

only one amino acid substitutions compared to six substitutions in the longitudinal interface (Arora et al., 2023). These differences, even when conservative, can influence the stability of protomers based on their interaction with the solvent and other protomer residues, potentially shifting filament flexibility and turnover rates . The overall D-loop topology is highly preserved, but its local environment can be influenced by substitutions in other subdomains, impacting D-loop flexibility and interactions, despite the fact that the D-loop sequence is identical between vertebrate isoforms (Arora et al., 2023).

These subtle but distinct molecular differences contribute to observed functional distinctions between isoforms including differential dynamics (e.g. β-actin polymerizes 1.5-fold faster than α-actin) and different biochemistries and interactions with myosin motors and ABPs (Ceron et al., 2022; Haarer et al., 2023). The latter leads to the formation of diverse cellular actin networks with distinct compositions, architectures, dynamics, and mechanics . For example, different myosin motors also show differential preferences for muscle or non-muscle actin, and some even distinguish between β- and γ-isoforms for movement (Müller et al., 2013). The isoform-specific interfaces likely fine-tune the enzymatic output of myosin motors for specialized cellular functions.

7.2. Actin mutations

Vertebrate actin isoforms are subject to pathogenic mutations linked to a broad spectrum of debilitating diseases (Parker et al., 2020). For instance, mutations in skeletal α-actin and cardiac α-actin are associated with muscle disorders such as nemaline myopathy and cardiomyopathies (Heissler and Chinthalapudi, 2025). Mutations in cytoplasmic β- and γ-actins have been linked to developmental malformations, deafness, and cancer (Parker et al., 2020). Disease-linked mutations can be distributed throughout the actin fold, affecting various inter-subunit contacts (Ceron et al., 2024). They frequently impact key structural regions critical for filament polymerization and stabilization including the D-loop, regions near the nucleotide-binding cleft, and inter-protomer interfaces (Huang et al., 2024). For instance, mutations in the H-plug region (a segment involved in interstrand interactions) can weaken subunit contacts, making filaments prone to disassembly (Pospich et al., 2017).

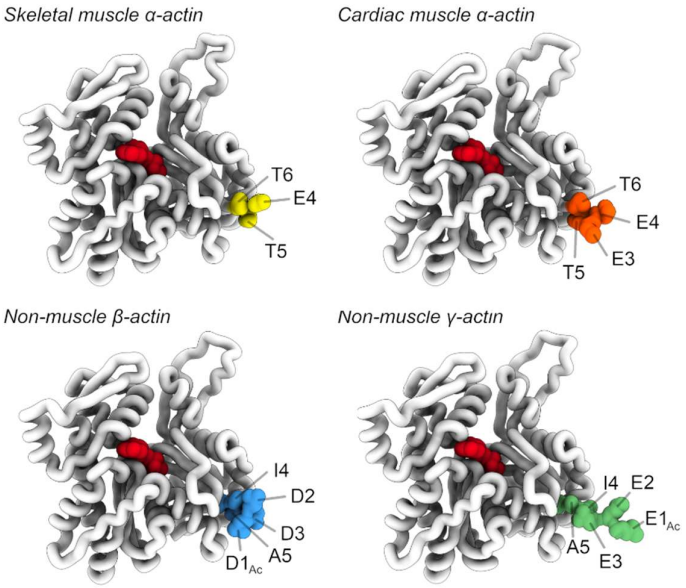

Figure 5. Structures of human actin isoforms. The bound nucleotide (ADP) is shown in red. N-terminal residues of α-skeletal, α-cardiac, β-, and γ-actin are highlighted in distinct colors, with individual residues labeled. The subscript "Ac" indicates acetylation.

 doi:10.20944/preprints202604.2036.v1

Cryo-EM studies consistently show that disease-causing mutations only induce subtle changes in the overall architecture of bare actin filaments (Ceron et al., 2024; Huang et al., 2024). However, small alterations at inter-subunit interfaces can profoundly impact filament stability and function with specific mutations directly impairing subunit-subunit contacts within the filament (Ceron et al., 2024). Mechanistically, some mutations act by promoting monomer sequestration, leading to their accumulation in cells rather than proper filament incorporation. Other mutations result in sluggish polymerization or generate short, unstable filaments prone to fragmentation (Ceron et al., 2024). These structural and dynamic perturbations manifest in altered polymerization kinetics.

Beyond altered polymerization dynamics, mutations can also affect filament mechanical properties or interactions with specific ABPs. For example, some mutations influence filament stiffness, as seen with the Y166S mutation in α-cardiac actin, which has been linked to altered cation-dependent stiffness and hypertrophic cardiomyopathy (Müller et al., 2012). Additionally, mutations can impact cofilin-mediated filament severability, such as the N111S substitution in β-actin. This mutation accelerates Pi release, thereby favoring the ADP state that cofilin preferentially binds for severing (Oosterheert et al., 2023)., potentially contributing to disease pathophysiology.

7.3. Evolutionary divergence of actin

Despite being one of the most conserved eukaryotic proteins, actin exhibits measurable divergence across evolutionary lineages (Pollard, 2016). For instance, Plasmodium falciparum actin (PfAct1) shares 82% sequence identity with human cytoplasmic γ-actin, marking it as one of the most divergent actins in the eukaryotic phylogenetic tree (Robert-Paganin et al., 2021). The core F-actin structure is broadly maintained across lineages (Pospich et al., 2017; Xu et al., 2024). However, specific regions often display more pronounced sequence variability, indicating an evolutionary tuning of binding compatibility rather than the core filament architecture itself (Pollard, 2016). One of the most affected regions is the D-loop. Generally, its conformation can shift between open and closed states (Merino et al., 2018), influenced by nucleotide state, mechanical forces, or the binding of ABPs.

In the Plasmodium falciparum actin PfAct1, the D-loop is shifted outward relative to vertebrate actin (Pospich et al., 2017; Kumpula et al., 2019), likely due to a kink introduced by the substitution of Q41 (in vertebrate actin) with proline (P42 in PfAct1), which also contributes to the inherent filament instability of PfAct1 (Lu et al., 2019). The PfAct1 D-loop is locked in the closed conformation independent even in the presence of JASP, which induces the open D-loop conformation in vertebrate actin independent of nucleotide state (Pospich et al., 2020). The presence of P42 is the likely cause that prevents the PfAct1 D-loop to adopt the open conformation. In the presence of PfMyoA, the Plasmodium myosin variant, the PfAct1 D-loop remains in place (Robert-Paganin et al., 2021), unlike what is observed with some mammalian actomyosins like NM2c, Myo6, or Myosin-15 (Robert-Paganin et al., 2021; Gong et al., 2022). The inability to adopt the open conformation, which is linked to increased stability in other actins, likely plays a role in the parasite's biology and the PfAct1 filament's short-lived nature.

The D-loop of Zea mays pollen plant actin (ZMPA) in the ADP state, like PfAct1, also bends farther outward compared to vertebrate actin (Ren et al., 2019). However, in contrast to PfAct1, it adopts an open conformation similar to JASP stabilized vertebrate filaments. This effectively means that the typical closed ADP-state D-loop seen in vertebrate actin is not observed in ZMPA under ADP-bound conditions, suggesting a unique inherent stability that is less influenced by the absence of Pi as would be the case in vertebrate actins (Merino et al., 2018).

The D-loop of Saccharomyces cerevisiae (yeast) actin filaments generally adopts a closed orientation similar to vertebrate actin in the ADP state, but with a slight reorientations and peptide flips to accommodate the alterations in the yeast-actin target-binding cleft (Xu et al., 2024). The yeast D-loop only has a single conservative sequence deviation compared to vertebrate actin and its conformation can be shifted by the A167E mutation, which is linked closely to magnesium ion binding and filament stiffness (Kang et al., 2013). This mutation induces a D-loop state closely resembling that of vertebrate actin, reversing the peptide flips observed in yeast (Xu et al., 2024).

 doi:10.20944/preprints202604.2036.v1

Beyond the D-loop, other variable regions important for actin dynamics include the H-plug (residues 263-273), which serves as a major interstrand contact whose electrostatic interactions contribute significantly to filament stability. In PfAct1 as well as leishmania actin substitutions in the H-plug region alter the electrostatics and weaken the interstrand contacts (Pospich et al., 2017; Kotila et al., 2022). In leishmania actin, hydrophobic contacts in the D-loop compensate for the weakening in the H-plug (Kotila et al., 2022).

The C-terminus (residues 349-375), which functions a nucleotide-sensing element that can be flexible or ordered coupled to the D-loop state and influenced by Pi release (Oosterheert et al., 2022), also shows variations between species. In vertebrate F-actin, the C-terminus typically folds into an α-helix in the closed D-loop state. In contrast to vertebrate actins, for PfAct1 the C-terminus is disordered in most crystal structures. However, specific mutations in PfAct1 (G115A or H74Q), can induce ordering in the C-terminus (Kumpula et al., 2019). This suggests that specific residues influence whether the C-terminus is ordered or not. JASP stabilizes the C-terminus in filamentous PfAct1 (Pospich et al., 2017).

The W-loop, located in SD3, is a region in the barbed groove that undergoes displacements during polymerization to facilitate D-loop interactions and to accommodate the stiffness cation (Xu et al., 2024) (Figure 3D). In the filament core, it forms a pincer-like structure with the C-terminus that grasps the D-loop of the subunit below (Carman et al., 2023). During polymerization, the W-loop (with Y169 at its tip) shifts from its monomer position toward the barbed end of the subunit (Chou and Pollard, 2019). This movement is crucial for allowing the D-loop to wrap around the knob formed by Y169 and for opening a hydrophobic pocket for the insertion of residue M44 from the D-loop of an adjacent subunit.

In yeast actin, the W-loop has sequence differences compared to vertebrate actin at three positions, including the knob residue Y169, which is substituted by a phenylalanine (Stevenson et al., 2025). Despite this sequence divergence, this region in yeast and vertebrate actin align almost perfectly locally but show a relative shift in the coordinate frame of the subunit (Xu et al., 2024). The A167E mutation in yeast induces a change in D-loop conformation, suggesting that the residue at position 167 (alanine in yeast vs. glutamic acid in vertebrates) is a primary determinant of the D-loop conformation, rather than D-loop sequence variations themselves (Xu et al., 2024). In Arp3, a component of the Arp2/3 complex, the W-loop (specifically residues 169-180) undergoes conformational changes associated with opening a hydrophobic pocket for binding the first daughter filament actin subunit in Arp2/3 complex branches (Chavali et al., 2024). This highlights how W-loop function extends beyond actin itself to actin-related proteins in mediating essential assembly processes.

Minor sequence differences at the subunit interfaces across species can lead to quantifiable differences in helical twist and subunit contact angles (Kotila et al., 2022). Both PfAct1 and yeast filaments are more tightly wound (helical twist of −167.5° and −167.2° respectively) as compared to the of vertebrate actins (helical twist of −166.6°) (Pospich et al., 2017; Xu et al., 2024). Although small on the level of individual actin subunits, over the typical length of a filament this difference in twist can significantly affect various cellular functions like myosin-based motility, crosslinker density in bundles, and interactions with severing proteins (Xu et al., 2024).

The evolutionary divergence in actin also manifests in its interactions with myosin motors. While there is a conserved core actomyosin interface common to all myosins across diverse phylogenetic branches (from apicomplexans to humans), ancillary interfaces provide specificity in track recognition (Robert-Paganin et al., 2021). These ancillary interfaces influence the motor

7.4. Actin-related proteins and actin-like homologues

The existence and diversity of actin-related proteins (Arps) and bacterial actin-like homologues (Alps) underscore the evolutionary plasticity of the actin fold (Merino and Raunser, 2016; Dominguez and Holmes, 2011). Arps originated from multiple duplications of a primordial actin gene early in eukaryotic evolution, diverging into distinct families with specialized functions over a billion years

 doi:10.20944/preprints202604.2036.v1

ago (Muller et al., 2005). They share 17% to 52% sequence identity with actin but retain the same fundamental fold, including the sites required for ATP binding (Pollard, 2016). Their surfaces, however, differ extensively from actin, often featuring insertions of surface loops and numerous amino acid substitutions that facilitate their formation of unique macromolecular assemblies (Muller et al., 2005). Examples include Arp1 and Arp11 in the dynactin complex, Arp2 and Arp3 of the Arp2/3 complex, and Arp4 through Arp9 in chromatin-remodeling complexes (Blessing et al., 2004).

Bacterial Alps also demonstrate this extensive evolutionary plasticity. MreB forms anti-parallel, double filaments and appears to lack a D-loop equivalent (van den Ent et al., 2014). ParM polymerizes with GTP and forms a filament with a left-handed long-pitch helix, contrasting with actin's right-handed helix, but includes a sequence resembling the D-loop (Galkin et al., 2009). AlfA represents a distinct class of Alps that polymerize very rapidly with either ATP or GTP (Rivera et al., 2011). These homologs, despite low sequence identity to eukaryotic actin, can form filaments surprisingly similar to F-actin (Merino and Raunser, 2016).

The combination of remarkable sequence conservation, subtle isoform-specific differences, and precise regulation by ABPs underlies actin's versatility in supporting diverse cellular processes. Cryo-EM continues to reveal how these factors intersect at atomic resolution, clarifying the structural basis of actin's dynamic behavior in health and disease.

8. Cellular Functions of Actin Filaments: In Situ Structure, Organization, and Dynamics

The transition from reconstituted actin systems to high-resolution structural work in intact cells has transformed our understanding of actin filament architecture and function (Chakraborty et al., 2020; Schneider and Jasnin, 2024; Hanein and Volkmann, 2024). While in vitro reconstitution defined much of the canonical actin framework, in situ studies, particularly cryo-electron tomography (cryo-ET) combined with subtomogram averaging (STA) have revealed that endogenous filaments occupy a far richer structural landscape. Subtle but functionally relevant deviations in filament twist, branch angle, spacing, and binding interfaces are common, and these features vary according to the architectural demands of the cellular environment.

8.1. Actin organization in lamellipodia

Lamellipodia are thin, sheet-like, dynamic cellular protrusions found at the leading edge of migrating cells. Lamellpodia are dominated by dense, dendritically branched actin arrays with the Arp2/3 complex acting as the primary nucleator responsible for generating these branched networks (Pollard and Borisy, 2003). Cryo-ET analyses have revealed that the in-situ branch angles are around 70° independent of cell type (Atherton et al., 2022; Jasnin et al., 2019; Fäßler et al., 2020; Anderson et al., 2016; Inaba et al., 2025; Chung et al., 2022). Subnanometer in-situ structures of the branch junction indicate that the branch angle is generally quite rigid in the lamellipodium with a narrow angular distribution (Fäßler et al., 2020), consistent with high-resolution in-vitro studies (Chou et al., 2022; Ding et al., 2022; Chavali et al., 2024). However, in the context of endocytosis and in comet-tails of listeria where Arp2/3-mediated branches are involved in force generation, angles can be significantly more varied with a standard deviation of about 10° (Serwas et al., 2022; Jasnin and Crevenna, 2015). This suggests that mechanical load can subtly bias the orientation of new branches from existing actin filaments. The Arp2/3 complex has also been observed to preferentially bind to bent actin filaments, and convex bends are favored for the initiation of new branches (Risca et al., 2012). This mechanism implies a direct link between force-response filament bending and the biasing of new branch formation.

The actin cytoskeleton in lamellipodia is characterized by a high proportion of filaments with their barbed ends facing the plasma membrane, which is consistent with their role in driving protrusive extension driven by Arp2/3 mediated branch formation (Pollard and Borisy, 2003). While about two thirds of filaments are-oriented in this way, significant populations of parallel and backward-oriented filaments also exist, at least in some cell types (Chung et al., 2022). The observed heterogeneity in actin filament orientation and polarity within different sub-domains of the

 doi:10.20944/preprints202604.2036.v1

lamellipodium suggests a more complex, dynamic reorganization of the actin network that contributes to protrusive extension than simple Arp2/3-mediated branching. Studies of cells lacking functional Arp2/3 show that protrusion and movement is supported without branch formation although the characteristic morphology of the leading edge is significantly altered (Anderson et al., 2016).

8.2. Actin organization in filopodia

Filopodia are thin, finger-like membrane protrusions that extend from the cell, functioning as dynamic antennae to sense and respond to external cues that influence cytoskeletal dynamics (Mattila and Lappalainen, 2008). Filopodia can exhibit remarkable geometric uniformity as they are primarily composed of parallel bundles of actin filaments, which are crosslinked predominantly by fascin (Faix and Rottner, 2006). These bundles are characterized by a uniform polarity, with actin filaments arranged in a characteristic hexagonal pseudo-crystalline array and an inter-filament distance of approximately 12 nm (Atherton et al., 2022; Jasnin et al., 2013; Gong et al., 2025; Yang et al., 2013). Filopodia can also exhibit more nuanced geometries at their tips, sometime referred to as terminal cone, with relatively short filaments that have no fixed spatial relationship (Medalia et al., 2007; Anderson et al., 2016). While the filaments in filopodia tend to point their barbed end towards the protruding membrane (Pollard, 2016), other morphologically thin protrusions such as pseudopodia in platelets (Sorrentino et al., 2021) can display mixed actin-filament polarity, hinting at a possible role of these protrusions in myosin-based force generation (Sorrentino et al., 2021). These findings emphasize that the local filament organization does not only depend on the macro-level morphology but also on the function of the protrusion.

The helical parameters of individual filaments within fascin-based bundles generally closely match canonical in vitro values, with fascin-cross-linked filaments showing a twist nearly identical to F-actin's canonical -166.7° (Gong et al., 2025). While many filaments maintain this canonical twist, slight variations can be detected, particularly at bundle tips where spacing expands to accommodate filament addition or bundle merging [(Atherton et al., 2022). A minority of filaments within these bundles can display a distinct appearance with a shorter helical repeat length of approximately 27 nm (Atherton et al., 2022), significantly shorter and therefore less tightly wound than the canonical 36 nm, consistent with cofilin binding (Huehn et al., 2020). That bundles stay intact even in the presence of twist modulations suggests that fascin, the primary crosslinker, possesses structural plasticity that enables flexible actin bundle construction (Gong et al., 2025). This tolerance for modest twist heterogeneity allows filopodia to curve and adapt without compromising bundle integrity, a characteristic crucial for their dynamic activities and shape maintenance in living cells.

8.3. Actin organization in contractile systems

In contractile systems, such as stress fibers, in situ reconstructions show a markedly different organization from filopodia or lamellipodia. Stress fibers are a prominent class of contractile actomyosin bundles that are composed of antiparallel bundles anchored at focal adhesion sites, playing a crucial role in sensing, generating, and transmitting tension to the extracellular matrix (Burridge and Wittchen, 2013). These structures are recognized as unbranched actin networks, with their assembly regulated by formins (Hotulainen and Lappalainen, 2006). Unlike filopodia which often show hexagonal packing, stress fibers tend to form sheets. Cryo-ET data suggest that these sheets are placed on top of each other, though in some instances, these sheets can also be hexagonally packed (Jasnin et al., 2013). The parallel filaments in stress fibers are generally less ordered and less densely packed compared to those in filopodia. This looser overall packing is thought to contribute to their flexibility, which is essential for their contractile function.

Perhaps the most dramatic example of an in-situ analysis of actin architectures in contractile systems comes from the study of skeletal muscle thin filaments bound to nebulin. Cryo-ET combined with sub-tomogram averaging resolved the detailed, near-atomic resolution structure of the F-actin/nebulin complex at 4.5-Å resolution (Wang et al., 2022). The structure resolves the continuous

 doi:10.20944/preprints202604.2036.v1

alignment of nebulin's ~35-residue repeats to the actin subunit repeat, forming a one-to-one registry across the entire filament. Nebulin-bound filaments in situ show that twist variations are suppressed to under ±0.3°, far lower than typical in vitro values (Wang et al., 2022). Tropomyosin co-occupies the same binding groove, but its position is slightly shifted compared to in vitro reconstructions, avoiding steric conflict with nebulin. Adjacent actin monomers physically separate nebulin from tropomyosin, regardless of tropomyosin (Marttila et al., 2014). These discrepancies between in-vitro and in-situ findings reemphasizes the importance of exploring structure in the full cellular context.

Taken together, these comparisons reveal that while the fundamental actin geometry defined in vitro provides the baseline, in situ structures are tuned by partner proteins, crowding, and mechanical history. Nebulin-bound filaments in muscle and azimuthally shifted actomyosin complexes in stress fibers exemplify extreme functional optimization, while more modest twist and branch-angle adjustments in lamellipodia and cortex show how mechanical adaptability can be built into the lattice. The consistency of certain parameters—such as the Arp2/3 branch angle remaining near 70°—underscores the robustness of core mechanisms, even as other features shift in response to the cellular context.

8.4. Actin network dynamics

Linking functional light microscopy (LM) studies to the nanoscale organization of actin filaments in cells is a critical step for a comprehensive understanding of cellular processes. While cryo-ET offers unparalleled resolution of cellular structures in situ, integrating these insights with dynamic, functional LM data presents both challenges and opportunities (Hanein and Volkmann, 2024). Despite significant advancements, cryo-ET for cytoskeletal studies is often constrained by several factors that limit its direct applicability in comprehensive cell biology: To link functional LM with cryo-ET data, correlative light and electron microscopy (CLEM) (Hanein and Volkmann, 2011) has become indispensable. This technique allows for the precise alignment of LM data, which captures dynamic cellular processes and protein localization, with the high-resolution structural details from cryo-ET of the same cellular region.

Tomographic data sets typically capture only a small area within a single eukaryotic cell, and their detailed analysis is resource and time intensive. This often leads studies to rely on a limited number of tomograms, making it difficult to generalize findings across diverse cellular regions, cell types, or over time. Additionally, the actin cytoskeleton is highly responsive to its cellular environment, with factors like substrate stiffness and extracellular matrix (ECM) composition significantly influencing actin organization (Gaietta et al., 2022). Many cryo-ET studies traditionally involve cells cultured directly on electron microscopy (EM) grids, sometimes without adequately replicating their native physiological environment. Automation of sample preparation and data collection (Tacke et al., 2021; Kuba et al., 2020; Chua et al., 2022), novel methods for providing more physiological environments (Gaietta et al., 2022), and accelerated computational analysis approaches (Volkmann, 2025) are beginning to address these bottlenecks.

A significant application of correlative approaches involves directly connecting high-resolution structural information with spatiotemporal signaling dynamics. For instance, a correlative spatiotemporal multiscale workflow was developed to unravel the initial organization of actin networks prompted by Rac1 activation (Marston et al., 2019). Rac1, a small GTPase, serves as a major upstream regulator of lamellipodia formation and influences cell motility, mechanosensing, and invasion by prompting the initial organization of actin networks (Hall, 1998). Live-cell imaging using a Förster Resonance Energy Transfer (FRET)-based Rac1 biosensor was used to generate spatiotemporal maps of Rac1 activation at the cell periphery. Subsequent cryo-ET scrutinized the nanoscale structure of the same region at a time point defined by the last live-cell imaging frame (Marston et al., 2019). Observations revealed that regions exhibiting recent high Rac1 activity exclusively featured densely packed, short actin filament structures, devoid of mutual alignment or branches. These distinctive actin assemblies were transient, becoming undetectable 150 seconds after Rac1 activity ceased (Marston et al., 2019). This approach directly translated the advent of Rac1

 doi:10.20944/preprints202604.2036.v1

activity into unique nanoscale cytoskeletal architecture. If Rac1 activity persists, lamellipodia with dendritic network architecture are formed (Inaba et al., 2025)

Another example of linking functional LM to high-resolution actin organization is the study of talin tension in peripheral focal adhesions (FAs) (Kumar et al., 2018). Talin is essential for force transmission between integrins and F-actin (Critchley, 2004). A combination of LM of talin tension sensors with cellular cryo-ET, researchers found a strong correlation: showed high actin filament alignment in regions with elevated talin tension, while areas with lower tension displayed significantly reduced alignment (Kumar et al., 2018). Quantification of filament order from tomograms was achieved using a novel Fourier-based method (Kumar et al., 2018; Volkmann, 2025), that completely bypasses the need for time-consuming and error-prone single-filament tracing and analysis, enabling high-throughput processing of tomographic data.

These correlative approaches allow to move beyond static structural images to understand the dynamic molecular mechanisms that govern actin network organization in various cellular contexts, offering a more quantitative and context-dependent understanding. By developing workflows that integrate high resolution cryo-EM with correlative light microscopy, we are beginning to reveal the native architectures of actin in situ and uncover how these structures relate to their functions and dynamics. This is only the beginning; much deeper insights are poised to emerge in the coming years, transforming our understanding of actin organization in its native cellular context.

Conclusions and Outlook

Actin forms the dynamic cytoskeleton essential for myriad cellular functions, from motility and shape maintenance to muscle contraction. Its diverse functions are orchestrated by a large repertoire of ABPs, which finely control polymerization, depolymerization, and network organization. Multiple actin isoforms, with subtle yet significant structural and biochemical differences, add another regulatory layer, shaping isoform-specific roles and ABP interactions.

Over the past decade, high-resolution cryo-EM has fundamentally transformed our understanding of actin. Near-atomic structures of F-actin in all nucleotide states (ATP, ADP-Pi, ADP) revealed the structural transitions underlying ATP hydrolysis and subsequent phosphate release. Detailed views of ABPs, including various myosins, nucleators, crosslinkers, papping, and severing proteins, have provided insights into their mechanisms of regulation. Structures of filament ends, both barbed and pointed, clarified fundamental aspects of growth and depolymerization, while additional studies illuminated structural plasticity of actin, such as filament bending and D-loop conformations.

Despite these advances, key questions remain. The precise molecular route of phosphate (Pi) release from F-actin is unresolved, as are the mechanisms by which ABPs detect nucleotide states and whether a unified sensing mechanism exists. Many ABP complexes remain difficult to capture in flexible, transient or active conformations. Moreover, the influence of post-translational modifications and disease-linked mutations on actin function requires systematic exploration.

The next frontier lies in in-situ structural biology. While in-vitro cryo-EM will remain critical for mechanistic dissection, cryo-ET, combined with cryo-focused ion beam (cryo-FIB) milling, correlative light and electron microscopy (CLEM), automated data acquisition and analysis, and advanced sample preparation techniques such as micropatterning, is opening an unprecedented window into actin within its native cellular context. By integrating structural snapshots with spatiotemporal dynamics, cryo-ET promises to link molecular resolution with cellular physiology. In essence, cryo-EM has revealed the molecular logic of purified actin and its complexes; cryo-ET now holds the potential to unravel how these insights translate into the living cell, offering a. holistic approach and dynamic picture of the actin cytoskeleton in biology and disease.

 doi:10.20944/preprints202604.2036.v1

Institutional Review Board Statement: Not applicable.

Informed Consent Statement: Not applicable.

Conflicts of Interest: The authors declare no conflict of interest.

References

1. Anderson, K. L., Page, C., Swift, M. F., Suraneni, P., Janssen, M. E. W., Pollard, T. D., Li, R., Volkmann, N., and Hanein, D. (2016). Nano-scale actin-network characterization of fibroblast cells lacking functional Arp2/3 complex. J Struct Biol *197*, 312-321.
2. Arora, A. S., Huang, H.-L., Singh, R., Narui, Y., Suchenko, A., Hatano, T., Heissler, S. M., Balasubramanian, M. K., and Chinthalapudi, K. (2023). Structural insights into actin isoforms. Elife *12*, e82015.
3. Atherton, J., Stouffer, M., Francis, F., and Moores, C. A. (2022). Visualising the cytoskeletal machinery in neuronal growth cones using cryo-electron tomography. J Cell Sci *135*, jcs259234.
4. Baltes, C., Thalla, D. G., Kazmaier, U., and Lautenschläger, F. (2022). Actin stabilization in cell migration. Front Cell Dev Biol *10*, 931880.
5. Banerjee, D. S., Freedman, S. L., Murrell, M. P., and Banerjee, S. (2024). Growth-induced collective bending and kinetic trapping of cytoskeletal filaments. Cytoskeleton (Hoboken) *81*, 409-419.
6. Barrie, K. R., Rebowski, G., and Dominguez, R. (2025). Mechanism of actin filament severing and capping by gelsolin. Nat Struct Mol Biol *32*, 237-242.
7. Belin, B. J., Goins, L. M., and Mullins, R. D. (2014). Comparative analysis of tools for live cell imaging of actin network architecture. Bioarchitecture *4*, 189-202.
8. Belyy, A., Merino, F., Sitsel, O., and Raunser, S. (2020). Structure of the Lifeact-F-actin complex. PLoS Biol *18*, e3000925.
9. Bibeau, J. P., Pandit, N. G., Gray, S., Shatery Nejad, N., Sindelar, C. V., Cao, W., and De La Cruz, E. M. (2023). Twist response of actin filaments. Proc Natl Acad Sci U S A *120*, e2208536120.
10. Biertümpfel, C., Yamada, Y., Vasquez-Montes, V., Truong, T. V., Cada, A. K., and Mizuno, N. (2025). Biochemical and structural bases for talin ABSs-F-actin interactions. Proc Natl Acad Sci U S A *122*, e2405922122.
11. Blanchoin, L., Amann, K. J., Higgs, H. N., Marchand, J. B., Kaiser, D. A., and Pollard, T. D. (2000). Direct observation of dendritic actin filament networks nucleated by Arp2/3 complex and WASP/Scar proteins. Nature *404*, 1007-11.
12. Blanchoin, L., Boujemaa-Paterski, R., Sykes, C., and Plastino, J. (2014). Actin dynamics, architecture, and mechanics in cell motility. Physiol Rev *94*, 235-263.
13. Blessing, C. A., Ugrinova, G. T., and Goodson, H. V. (2004). Actin and ARPs: action in the nucleus. Trends Cell Biol *14*, 435-442.
14. Boiero Sanders, M., Oosterheert, W., Hofnagel, O., Bieling, P., and Raunser, S. (2024). Phalloidin and DNase I-bound F-actin pointed end structures reveal principles of filament stabilization and disassembly. Nat Commun *15*, 7969.
15. Buckley, C. D., Tan, J., Anderson, K. L., Hanein, D., Volkmann, N., Weis, W. I., Nelson, W. J., and Dunn, A. R. (2014). Cell adhesion. The minimal cadherin-catenin complex binds to actin filaments under force. Science *346*, 1254211.
16. Burridge, K., and Wittchen, E. S. (2013). The tension mounts: stress fibers as force-generating mechanotransducers. J Cell Biol *200*, 9-19.
17. Carman, P. J., Barrie, K. R., Rebowski, G., and Dominguez, R. (2023). Structures of the free and capped ends of the actin filament. Science *380*, 1287-1292.
18. Ceron, R. H., Báez-Cruz, F. A., Palmer, N. J., Carman, P. J., Boczkowska, M., Heuckeroth, R. O., Ostap, E. M., and Dominguez, R. (2024). Molecular mechanisms linking missense ACTG2 mutations to visceral myopathy. Sci Adv *10*, eadn6615.
19. Ceron, R. H., Carman, P. J., Rebowski, G., Boczkowska, M., Heuckeroth, R. O., and Dominguez, R. (2022). A solution to the long-standing problem of actin expression and purification. Proc Natl Acad Sci U S A *119*, e2209150119.

 doi:10.20944/preprints202604.2036.v1

20. Chakraborty, S., Jasnin, M., and Baumeister, W. (2020). Three-dimensional organization of the cytoskeleton: A cryo-electron tomography perspective. Protein Sci *29*, 1302-1320.
21. Chavali, S. S., Chou, S. Z., Cao, W., Pollard, T. D., De La Cruz, E. M., and Sindelar, C. V. (2024). Cryo-EM structures reveal how phosphate release from Arp3 weakens actin filament branches formed by Arp2/3 complex. Nat Commun *15*, 2059.
22. Chou, S. Z., Chatterjee, M., and Pollard, T. D. (2022). Mechanism of actin filament branch formation by Arp2/3 complex revealed by a high-resolution cryo-EM structureof the branch junction. Proc Natl Acad Sci U S A *119*, e2206722119.
23. Chou, S. Z., and Pollard, T. D. (2019). Mechanism of actin polymerization revealed by cryo-EM structures of actin filaments with three different bound nucleotides. Proc Natl Acad Sci U S A *116*, 4265-4274.
24. Chou, S. Z., and Pollard, T. D. (2020). Cryo-electron microscopy structures of pyrene-labeled ADP-P_i- and ADP-actin filaments. Nat Commun *11*, 5897.
25. Chu, J.-W., and Voth, G. A. (2005). Allostery of actin filaments: molecular dynamics simulations and coarse-grained analysis. Proc Natl Acad Sci U S A *102*, 13111-13116.
26. Chua, E. Y. D., Mendez, J. H., Rapp, M., Ilca, S. L., Tan, Y. Z., Maruthi, K., Kuang, H., Zimanyi, C. M., Cheng, A., Eng, E. T., Noble, A. J., Potter, C. S., and Carragher, B. (2022). Better, Faster, Cheaper: Recent Advances in Cryo-Electron Microscopy. Annu Rev Biochem *91*, 1-32.
27. Chung, W.-L., Eibauer, M., Li, W., Boujemaa-Paterski, R., Geiger, B., and Medalia, O. (2022). A network of mixed actin polarity in the leading edge of spreading cells. Commun Biol *5*, 1338.
28. Courtemanche, N., and Henty-Ridilla, J. L. (2024). Actin filament dynamics at barbed ends: New structures, new insights. Curr Opin Cell Biol *90*, 102419.
29. Critchley, D. R. (2004). Cytoskeletal proteins talin and vinculin in integrin-mediated adhesion. Biochem Soc Trans *32*, 831-836.
30. Critchley, D. R. (2009). Biochemical and structural properties of the integrin-associated cytoskeletal protein talin. Annu Rev Biophys *38*, 235-254.
31. Das, S., Ge, P., Oztug Durer, Z. A., Grintsevich, E. E., Zhou, Z. H., and Reisler, E. (2020). D-loop Dynamics and Near-Atomic-Resolution Cryo-EM Structure of Phalloidin-Bound F-Actin. Structure *28*, 586-593.e3.
32. De La Cruz, E. M., and Gardel, M. L. (2015). Actin Mechanics and Fragmentation. J Biol Chem *290*, 17137-17144.
33. Ding, B., Narvaez-Ortiz, H. Y., Singh, Y., Hocky, G. M., Chowdhury, S., and Nolen, B. J. (2022). Structure of Arp2/3 complex at a branched actin filament junction resolved by single-particle cryo-electron microscopy. Proc Natl Acad Sci U S A *119*, e2202723119.
34. Dominguez, R. (2004). Actin-binding proteins--a unifying hypothesis. Trends Biochem Sci *29*, 572-578.
35. Dominguez, R. (2019). Nucleotide-dependent conformational changes in the actin filament: Subtler than expected. Proc Natl Acad Sci U S A
36. Dominguez, R., and Holmes, K. C. (2011). Actin structure and function. Annu Rev Biophys *40*, 169-186.
37. Drazic, A., Aksnes, H., Marie, M., Boczkowska, M., Varland, S., Timmerman, E., Foyn, H., Glomnes, N., Rebowski, G., Impens, F., Gevaert, K., Dominguez, R., and Arnesen, T. (2018). NAA80 is actin's N-terminal acetyltransferase and regulates cytoskeleton assembly and cell motility. Proc Natl Acad Sci U S A *115*, 4399-4404.
38. Durer, Z. A. O., Kudryashov, D. S., Sawaya, M. R., Altenbach, C., Hubbell, W., and Reisler, E. (2012). Structural states and dynamics of the D-loop in actin. Biophys J *103*, 930-939.
39. Egelman, E. H., Francis, N., and DeRosier, D. J. (1982). F-actin is a helix with a random variable twist. Nature *298*, 131-135.
40. Elam, W. A., Cao, W., Kang, H., Huehn, A., Hocky, G. M., Prochniewicz, E., Schramm, A. C., Negrón, K., Garcia, J., Bonello, T. T., Gunning, P. W., Thomas, D. D., Voth, G. A., Sindelar, C. V., and De La Cruz, E. M. (2017). Phosphomimetic S3D cofilin binds but only weakly severs actin filaments. J Biol Chem *292*, 19565-19579.
41. Faix, J., and Rottner, K. (2006). The making of filopodia. Curr Opin Cell Biol *18*, 18-25.
42. Fäßler, F., Dimchev, G., Hodirnau, V. V., Wan, W., and Schur, F. K. M. (2020). Cryo-electron tomography structure of Arp2/3 complex in cells reveals new insights into the branch junction. Nat Commun *11*, 6437.

 doi:10.20944/preprints202604.2036.v1

43. Fischer, R. S., and Fowler, V. M. (2003). Tropomodulins: life at the slow end. Trends Cell Biol *13*, 593-601.
44. Fowler, V. M. (1996). Regulation of actin filament length in erythrocytes and striated muscle. Curr Opin Cell Biol *8*, 86-96.
45. Gaietta, G., Kai, F., Swift, M. F., Weaver, V. M., Volkmann, N., and Hanein, D. (2022). Novel cryo-tomography workflow reveals nanometer-scale responses of epithelial cells to matrix stiffness and dimensionality. Mol Biol Cell mbcE22030092.
46. Galkin, V. E., Orlova, A., Kudryashov, D. S., Solodukhin, A., Reisler, E., Schröder, G. F., and Egelman, E. H. (2011). Remodeling of actin filaments by ADF/cofilin proteins. Proc Natl Acad Sci U S A *108*, 20568-20572.
47. Galkin, V. E., Orlova, A., Rivera, C., Mullins, R. D., and Egelman, E. H. (2009). Structural polymorphism of the ParM filament and dynamic instability. Structure *17*, 1253-1264.
48. Gittes, F., Mickey, B., Nettleton, J., and Howard, J. (1993). Flexural rigidity of microtubules and actin filaments measured from thermal fluctuations in shape. J Cell Biol *120*, 923-934.
49. Gong, R., Jiang, F., Moreland, Z. G., Reynolds, M. J., de Los Reyes, S. E., Gurel, P., Shams, A., Heidings, J. B., Bowl, M. R., Bird, J. E., and Alushin, G. M. (2022). Structural basis for tunable control of actin dynamics by myosin-15 in mechanosensory stereocilia. Sci Adv *8*, eabl4733.
50. Gong, R., Reynolds, M. J., Carney, K. R., Hamilton, K., Bidone, T. C., and Alushin, G. M. (2025). Fascin structural plasticity mediates flexible actin bundle construction. Nat Struct Mol Biol *32*, 940-952.
51. Goode, B. L., Eskin, J., and Shekhar, S. (2023). Mechanisms of actin disassembly and turnover. J Cell Biol *222*, e202309021.
52. Grintsevich, E. E., Ge, P., Sawaya, M. R., Yesilyurt, H. G., Terman, J. R., Zhou, Z. H., and Reisler, E. (2017). Catastrophic disassembly of actin filaments via Mical-mediated oxidation. Nat Commun *8*, 2183.
53. Gunning, P. W., Hardeman, E. C., Lappalainen, P., and Mulvihill, D. P. (2015a). Tropomyosin - master regulator of actin filament function in the cytoskeleton. J Cell Sci *128*, 2965-2974.
54. Gunning, P. W., Ghoshdastider, U., Whitaker, S., Popp, D., and Robinson, R. C. (2015b). The evolution of compositionally and functionally distinct actin filaments. J Cell Sci *128*, 2009-2019.
55. Guo, Q., Liao, S., Kwiatkowski, S., Tomaka, W., Yu, H., Wu, G., Tu, X., Min, J., Drozak, J., and Xu, C. (2019). Structural insights into SETD3-mediated histidine methylation on β-actin. Elife *8*, e43676.
56. Haarer, B. K., Pimm, M. L., de Jong, E. P., Amberg, D. C., and Henty-Ridilla, J. L. (2023). Purification of human β- and γ-actin from budding yeast. J Cell Sci *136*, jcs260540.
57. Hall, A. (1998). Rho GTPases and the actin cytoskeleton. Science *279*, 509-514.
58. Hanein, D., and Volkmann, N. (2011). Correlative light-electron microscopy. Adv Protein Chem Struct Biol *82*, 91-99.
59. Hanein, D., and Volkmann, N. (2024). Functional Studies of the Actin Cytoskeleton by Cryogenic Electron Tomography. In Cryo-Electron Microscopy in Structural Biology, Appasani, K., ed. (Boca Raton: CRC Press),
60. Heissler, S. M., and Chinthalapudi, K. (2025). Structural and functional mechanisms of actin isoforms. FEBS J *292*, 468-482.
61. Hightower, R. C., and Meagher, R. B. (1986). The molecular evolution of actin. Genetics *114*, 315-332.
62. Holmes, K. C., Popp, D., Gebhard, W., and Kabsch, W. (1990). Atomic model of the actin filament. Nature *347*, 44-49.
63. Hotulainen, P., and Lappalainen, P. (2006). Stress fibers are generated by two distinct actin assembly mechanisms in motile cells. J Cell Biol *173*, 383-394.
64. Huang, D. L., Bax, N. A., Buckley, C. D., Weis, W. I., and Dunn, A. R. (2017). Vinculin forms a directionally asymmetric catch bond with F-actin. Science *357*, 703-706.
65. Huang, H.-L., Suchenko, A., Grandinetti, G., Balasubramanian, M. K., Chinthalapudi, K., and Heissler, S. M. (2024). Cryo-EM structures of cardiac muscle α-actin mutants M305L and A331P give insights into the structural mechanisms of hypertrophic cardiomyopathy. Eur J Cell Biol *103*, 151460.
66. Huehn, A., Cao, W., Elam, W. A., Liu, X., De La Cruz, E. M., and Sindelar, C. V. (2018). The actin filament twist changes abruptly at boundaries between bare and cofilin-decorated segments. J Biol Chem

 doi:10.20944/preprints202604.2036.v1

67. Huehn, A. R., Bibeau, J. P., Schramm, A. C., Cao, W., De La Cruz, E. M., and Sindelar, C. V. (2020). Structures of cofilin-induced structural changes reveal local and asymmetric perturbations of actin filaments. Proc Natl Acad Sci U S A *117*, 1478-1484.
68. Huxley, H. E. (1963). Electron microscope studies on the structure of natural and synthetic protein filaments from striated muscle. J Mol Biol *7*, 281-308.
69. Inaba, H., Imasaki, T., Aoyama, K., Yoshihara, S., Takazaki, H., Kato, T., Goto, H., Mitsuoka, K., Nitta, R., and Nakata, T. (2025). Cryo-ET of actin cytoskeleton and membrane structure in lamellipodia formation using optogenetics. iScience *28*, 112529.
70. Iwamoto, D. V., Huehn, A., Simon, B., Huet-Calderwood, C., Baldassarre, M., Sindelar, C. V., and Calderwood, D. A. (2018). Structural basis of the filamin A actin-binding domain interaction with F-actin. Nat Struct Mol Biol *25*, 918-927.
71. Jasnin, M., Beck, F., Ecke, M., Fukuda, Y., Martinez-Sanchez, A., Baumeister, W., and Gerisch, G. (2019). The Architecture of Traveling Actin Waves Revealed by Cryo-Electron Tomography. Structure *27*, 1211-1223.e5.
72. Jasnin, M., Asano, S., Gouin, E., Hegerl, R., Plitzko, J. M., Villa, E., Cossart, P., and Baumeister, W. (2013). Three-dimensional architecture of actin filaments in Listeria monocytogenes comet tails. Proc Natl Acad Sci U S A *110*, 20521-20526.
73. Jasnin, M., and Crevenna, A. H. (2015). Quantitative Analysis of Filament Branch Orientation in Listeria Actin Comet Tails. Biophys J
74. Kabsch, W., Mannherz, H. G., Suck, D., Pai, E. F., and Holmes, K. C. (1990). Atomic structure of the actin:DNase I complex. Nature *347*, 37-44.
75. Kanematsu, Y., Narita, A., Oda, T., Koike, R., Ota, M., Takano, Y., Moritsugu, K., Fujiwara, I., Tanaka, K., Komatsu, H., Nagae, T., Watanabe, N., Iwasa, M., Maéda, Y., and Takeda, S. (2022). Structures and mechanisms of actin ATP hydrolysis. Proc Natl Acad Sci U S A *119*, e2122641119.
76. Kang, H., Bradley, M. J., Elam, W. A., and De La Cruz, E. M. (2013). Regulation of actin by ion-linked equilibria. Biophys J *105*, 2621-2628.
77. Klebl, D. P., McMillan, S. N., Risi, C., Forgacs, E., Virok, B., Atherton, J. L., Harris, S. A., Stofella, M., Winkelmann, D. A., Sobott, F., Galkin, V. E., Knight, P. J., Muench, S. P., Scarff, C. A., and White, H. D. (2025). Swinging lever mechanism of myosin directly shown by time-resolved cryo-EM. Nature *642*, 519-526.
78. Korn, E. D., Carlier, M. F., and Pantaloni, D. (1987). Actin polymerization and ATP hydrolysis. Science *238*, 638-644.
79. Kotila, T., Wioland, H., Selvaraj, M., Kogan, K., Antenucci, L., Jégou, A., Huiskonen, J. T., Romet-Lemonne, G., and Lappalainen, P. (2022). Structural basis of rapid actin dynamics in the evolutionarily divergent Leishmania parasite. Nat Commun *13*, 3442.
80. Kuba, J., Mitchels, J., Hovorka, M., Erdmann, P., Berka, L., Kirmse, R., KÖnig, J., DE Bock, J., Goetze, B., and Rigort, A. (2020). Advanced cryo-tomography workflow developments - correlative microscopy, milling automation and cryo-lift-out. J Microsc
81. Kumar, A., Anderson, K. L., Swift, M. F., Hanein, D., Volkmann, N., and Schwartz, M. A. (2018). Local Tension on Talin in Focal Adhesions Correlates with F-Actin Alignment at the Nanometer Scale. Biophys J *115*, 1569-1579.
82. Kumari, A., Kesarwani, S., Javoor, M. G., Vinothkumar, K. R., and Sirajuddin, M. (2020). Structural insights into actin filament recognition by commonly used cellular actin markers. EMBO J *39*, e104006.
83. Kumpula, E. P., Lopez, A. J., Tajedin, L., Han, H., and Kursula, I. (2019). Atomic view into Plasmodium actin polymerization, ATP hydrolysis, and fragmentation. PLoS Biol *17*, e3000315.
84. Lappalainen, P. (2016). Actin-binding proteins: the long road to understanding the dynamic landscape of cellular actin networks. Mol Biol Cell *27*, 2519-2522.
85. Li, N., Chen, S., Xu, K., He, M.-T., Dong, M.-Q., Zhang, Q. C., and Gao, N. (2023). Structural basis of membrane skeleton organization in red blood cells. Cell *186*, 1912-1929.e18.
86. Lu, H., Fagnant, P. M., and Trybus, K. M. (2019). Unusual dynamics of the divergent malaria parasite PfAct1 actin filament. Proc Natl Acad Sci U S A *116*, 20418-20427.

 doi:10.20944/preprints202604.2036.v1

87. Lyons, B., Mogre, S. S., Vegesna, K., Yu, J. S., Hansen, M., Raghunathan, A., Johnson, G. T., Agmon, E., and Akamatsu, M. (2025). Comparing simulations of actin filament compression reveals tradeoff between computational cost and capturing supertwist. MicroPubl Biol *2025*,
88. Marantan, A., and Mahadevan, L. (2018). Mechanics and statistics of the worm-like chain. American Journal of Physics *86*, 86-94.
89. Marston, D. J., Anderson, K. L., Swift, M. F., Rougie, M., Page, C., Hahn, K. M., Volkmann, N., and Hanein, D. (2019). High Rac1 activity is functionally translated into cytosolic structures with unique nanoscale cytoskeletal architecture. Proc Natl Acad Sci U S A *116*, 1267-1272.
90. Marttila, M., Hanif, M., Lemola, E., Nowak, K. J., Laitila, J., Grönholm, M., Wallgren-Pettersson, C., and Pelin, K. (2014). Nebulin interactions with actin and tropomyosin are altered by disease-causing mutations. Skelet Muscle *4*, 15.
91. Mattila, P. K., and Lappalainen, P. (2008). Filopodia: molecular architecture and cellular functions. Nat Rev Mol Cell Biol *9*, 446-454.
92. McCullagh, M., Saunders, M. G., and Voth, G. A. (2014). Unraveling the mystery of ATP hydrolysis in actin filaments. J Am Chem Soc *136*, 13053-13058.
93. McGough, A. (1998). F-actin-binding proteins. Curr Opin Struct Biol *8*, 166-176.
94. Medalia, O., Beck, M., Ecke, M., Weber, I., Neujahr, R., Baumeister, W., and Gerisch, G. (2007). Organization of actin networks in intact filopodia. Curr Biol *17*, 79-84.
95. Meenakshi S, I., Rao, M., Mayor, S., and Sowdhamini, R. (2023). A census of actin-associated proteins in humans. Front Cell Dev Biol *11*, 1168050.
96. Mei, L., Espinosa de Los Reyes, S., Reynolds, M. J., Leicher, R., Liu, S., and Alushin, G. M. (2020). Molecular mechanism for direct actin force-sensing by α-catenin. Elife *9*, e62514.
97. Mei, L., Reynolds, M. J., Garbett, D., Gong, R., Meyer, T., and Alushin, G. M. (2022). Structural mechanism for bidirectional actin cross-linking by T-plastin. Proc Natl Acad Sci U S A *119*, e2205370119.
98. Melki, R., Fievez, S., and Carlier, M. F. (1996). Continuous monitoring of Pi release following nucleotide hydrolysis in actin or tubulin assembly using 2-amino-6-mercapto-7-methylpurine ribonucleoside and purine-nucleoside phosphorylase as an enzyme-linked assay. Biochemistry *35*, 12038-12045.
99. Merino, F., Pospich, S., Funk, J., Wagner, T., Küllmer, F., Arndt, H. D., Bieling, P., and Raunser, S. (2018). Structural transitions of F-actin upon ATP hydrolysis at near-atomic resolution revealed by cryo-EM. Nat Struct Mol Biol *25*, 528-537.
100. Merino, F., Pospich, S., and Raunser, S. (2020). Towards a structural understanding of the remodeling of the actin cytoskeleton. Semin Cell Dev Biol *102*, 51-64.
101. Merino, F., and Raunser, S. (2016). The mother of all actins. Elife *5*,
102. Muller, J., Oma, Y., Vallar, L., Friederich, E., Poch, O., and Winsor, B. (2005). Sequence and comparative genomic analysis of actin-related proteins. Mol Biol Cell *16*, 5736-5748.
103. Müller, M., Mazur, A. J., Behrmann, E., Diensthuber, R. P., Radke, M. B., Qu, Z., Littwitz, C., Raunser, S., Schoenenberger, C. A., Manstein, D. J., and Mannherz, H. G. (2012). Functional characterization of the human α-cardiac actin mutations Y166C and M305L involved in hypertrophic cardiomyopathy. Cell Mol Life Sci *69*, 3457-3479.
104. Müller, M., Diensthuber, R. P., Chizhov, I., Claus, P., Heissler, S. M., Preller, M., Taft, M. H., and Manstein, D. J. (2013). Distinct functional interactions between actin isoforms and nonsarcomeric myosins. PLoS One *8*, e70636.
105. Niedzialkowska, E., Runyan, L. A., Kudryashova, E., Egelman, E. H., and Kudryashov, D. S. (2024). Stabilization of F-actin by Salmonella effector SipA resembles the structural effects of inorganic phosphate and phalloidin. Structure *32*, 725-738.e8.
106. Oda, T., Iwasa, M., Aihara, T., Maeda, Y., and Narita, A. (2009). The nature of the globular- to fibrous-actin transition. Nature *457*, 441-445.
107. Oosterheert, W., Blanc, F. E. C., Roy, A., Belyy, A., Sanders, M. B., Hofnagel, O., Hummer, G., Bieling, P., and Raunser, S. (2023). Molecular mechanisms of inorganic-phosphate release from the core and barbed end of actin filaments. Nat Struct Mol Biol *30*, 1774-1785.

 doi:10.20944/preprints202604.2036.v1

108. Oosterheert, W., Boiero Sanders, M., Bieling, P., and Raunser, S. (2025). Structural insights into actin filament turnover. Trends Cell Biol S0962-8924(24)00277.
109. Oosterheert, W., Boiero Sanders, M., Funk, J., Prumbaum, D., Raunser, S., and Bieling, P. (2024). Molecular mechanism of actin filament elongation by formins. Science *384*, eadn9560.
110. Oosterheert, W., Klink, B. U., Belyy, A., Pospich, S., and Raunser, S. (2022). Structural basis of actin filament assembly and aging. Nature 1-6.
111. Owen, L. M., Bax, N. A., Weis, W. I., and Dunn, A. R. (2022). The C-terminal actin-binding domain of talin forms an asymmetric catch bond with F-actin. Proc Natl Acad Sci U S A *119*, e2109329119.
112. Parker, F., Baboolal, T. G., and Peckham, M. (2020). Actin Mutations and Their Role in Disease. Int J Mol Sci *21*, 3371.
113. Perrin, B. J., and Ervasti, J. M. (2010). The actin gene family: function follows isoform. Cytoskeleton (Hoboken) *67*, 630-634.
114. Podolski, J. L., and Steck, T. L. (1990). Length distribution of F-actin in Dictyostelium discoideum. J Biol Chem *265*, 1312-1318.
115. Pollard, T. D. (1986). Rate constants for the reactions of ATP- and ADP-actin with the ends of actin filaments. J Cell Biol *103*, 2747-2754.
116. Pollard, T. D., Blanchoin, L., and Mullins, R. D. (2000). Molecular mechanisms controlling actin filament dynamics in nonmuscle cells. Annu Rev Biophys Biomol Struct *29*, 545-76.
117. Pollard, T. D., and Borisy, G. G. (2003). Cellular motility driven by assembly and disassembly of actin filaments. Cell *112*, 453-65.
118. Pollard, T. D. (2016). Actin and Actin-Binding Proteins. Cold Spring Harb Perspect Biol
119. Pospich, S., Kumpula, E. P., von der Ecken, J., Vahokoski, J., Kursula, I., and Raunser, S. (2017). Near-atomic structure of jasplakinolide-stabilized malaria parasite F-actin reveals the structural basis of filament instability. Proc Natl Acad Sci U S A *114*, 10636-10641.
120. Pospich, S., Merino, F., and Raunser, S. (2020). Structural Effects and Functional Implications of Phalloidin and Jasplakinolide Binding to Actin Filaments. Structure *28*, 437-449.e5.
121. Pospich, S., Sweeney, H. L., Houdusse, A., and Raunser, S. (2021). High-resolution structures of the actomyosin-V complex in three nucleotide states provide insights into the force generation mechanism. Elife *10*, e73724.
122. Prochniewicz, E., Janson, N., Thomas, D. D., and De la Cruz, E. M. (2005). Cofilin increases the torsional flexibility and dynamics of actin filaments. J Mol Biol *353*, 990-1000.
123. Rall, J. A. (2018). Generation of life in a test tube: Albert Szent-Gyorgyi, Bruno Straub, and the discovery of actin. Adv Physiol Educ *42*, 277-288.
124. Rebowski, G., Boczkowska, M., Drazic, A., Ree, R., Goris, M., Arnesen, T., and Dominguez, R. (2020). Mechanism of actin N-terminal acetylation. Sci Adv *6*, eaay8793.
125. Ren, Z., Zhang, Y., Zhang, Y., He, Y., Du, P., Wang, Z., Sun, F., and Ren, H. (2019). Cryo-EM Structure of Actin Filaments from Zea mays Pollen. Plant Cell *31*, 2855-2867.
126. Reynolds, M. J., Hachicho, C., Carl, A. G., Gong, R., and Alushin, G. M. (2022). Bending forces and nucleotide state jointly regulate F-actin structure. Nature *611*, 380-386.
127. Riedl, J., Crevenna, A. H., Kessenbrock, K., Yu, J. H., Neukirchen, D., Bista, M., Bradke, F., Jenne, D., Holak, T. A., Werb, Z., Sixt, M., and Wedlich-Soldner, R. (2008). Lifeact: a versatile marker to visualize F-actin. Nat Methods *5*, 605-607.
128. Risca, V. I., Wang, E. B., Chaudhuri, O., Chia, J. J., Geissler, P. L., and Fletcher, D. A. (2012). Actin filament curvature biases branching direction. Proc Natl Acad Sci U S A *109*, 2913-2918.
129. Risi, C. M., Belknap, B., Atherton, J., Coscarella, I. L., White, H. D., Bryant Chase, P., Pinto, J. R., and Galkin, V. E. (2024). Troponin Structural Dynamics in the Native Cardiac Thin Filament Revealed by Cryo Electron Microscopy. J Mol Biol *436*, 168498.
130. Rivera, C. R., Kollman, J. M., Polka, J. K., Agard, D. A., and Mullins, R. D. (2011). Architecture and assembly of a divergent member of the ParM family of bacterial actin-like proteins. J Biol Chem *286*, 14282-14290.
131. Robert-Paganin, J., Pylypenko, O., Kikuti, C., Sweeney, H. L., and Houdusse, A. (2020). Force Generation by Myosin Motors: A Structural Perspective. Chem Rev *120*, 5-35.

 doi:10.20944/preprints202604.2036.v1

132. Robert-Paganin, J., Xu, X. P., Swift, M. F., Auguin, D., Robblee, J. P., Lu, H., Fagnant, P. M., Krementsova, E. B., Trybus, K. M., Houdusse, A., Volkmann, N., and Hanein, D. (2021). The actomyosin interface contains an evolutionary conserved core and an ancillary interface involved in specificity. Nat Commun *12*, 1892.
133. Schneider, J., and Jasnin, M. (2024). Molecular architecture of the actin cytoskeleton: From single cells to whole organisms using cryo-electron tomography. Curr Opin Cell Biol *88*, 102356.
134. Serwas, D., Akamatsu, M., Moayed, A., Vegesna, K., Vasan, R., Hill, J. M., Schöneberg, J., Davies, K. M., Rangamani, P., and Drubin, D. G. (2022). Mechanistic insights into actin force generation during vesicle formation from cryo-electron tomography. Dev Cell *57*, 1132-1145.e5.
135. Shaaban, M., Chowdhury, S., and Nolen, B. J. (2020). Cryo-EM reveals the transition of Arp2/3 complex from inactive to nucleation-competent state. Nat Struct Mol Biol *27*, 1009-1016.
136. Shatskiy, D., Sivan, A., Wedlich-Söldner, R., and Belyy, A. (2025). Structure of the F-tractin-F-actin complex. J Cell Biol *224*, e202409192.
137. Sorrentino, S., Conesa, J. J., Cuervo, A., Melero, R., Martins, B., Fernandez-Gimenez, E., de Isidro-Gomez, F. P., de la Morena, J., Studt, J.-D., Sorzano, C. O. S., Eibauer, M., Carazo, J. M., and Medalia, O. (2021). Structural analysis of receptors and actin polarity in platelet protrusions. Proc Natl Acad Sci U S A *118*, e2105004118.
138. Stevenson, S. R., Tzokov, S. B., Lahiri, I., Ayscough, K. R., and Bullough, P. A. (2025). Cryo-EM reconstruction of yeast ADP-actin filament at 2.5 Å resolution. A comparison with vertebrate F-actin. Structure *33*, 435-442.e3.
139. Stoddard, P. R., Williams, T. A., Garner, E., and Baum, B. (2017). Evolution of polymer formation within the actin superfamily. Mol Biol Cell *28*, 2461-2469.
140. Tacke, S., Erdmann, P., Wang, Z., Klumpe, S., Grange, M., Plitzko, J., and Raunser, S. (2021). A streamlined workflow for automated cryo focused ion beam milling. J Struct Biol *213*, 107743.
141. Terman, J. R., and Kashina, A. (2013). Post-translational modification and regulation of actin. Curr Opin Cell Biol *25*, 30-38.
142. Tseng, Y., Kole, T. P., Lee, J. S. H., Fedorov, E., Almo, S. C., Schafer, B. W., and Wirtz, D. (2005). How actin crosslinking and bundling proteins cooperate to generate an enhanced cell mechanical response. Biochem Biophys Res Commun *334*, 183-192.
143. Tsuda, Y., Yasutake, H., Ishijima, A., and Yanagida, T. (1996). Torsional rigidity of single actin filaments and actin-actin bond breaking force under torsion measured directly by in vitro micromanipulation. Proc Natl Acad Sci U S A *93*, 12937-12942.
144. van den Ent, F., Izoré, T., Bharat, T. A., Johnson, C. M., and Löwe, J. (2014). Bacterial actin MreB forms antiparallel double filaments. Elife *3*, e02634.
145. Varland, S., Vandekerckhove, J., and Drazic, A. (2019). Actin Post-translational Modifications: The Cinderella of Cytoskeletal Control. Trends Biochem Sci *44*, 502-516.
146. Volkmann, N. (2025). Interpretation of cellular tomograms. In Cryo-electron Tomography: A Journey from Sample Preparation to Data Mining, Hanein, D., and N. Volkmann, eds. (London: Academic Press),
147. Volkmann, N., Amann, K. J., Stoilova-McPhie, S., Egile, C., Winter, D. C., Hazelwood, L., Heuser, J. E., Li, R., Pollard, T. D., and Hanein, D. (2001). Structure of Arp2/3 complex in its activated state and in actin filament branch junctions. Science *293*, 2456-2459.
148. Volkmann, N., Page, C., Li, R., and Hanein, D. (2014). Three-dimensional reconstructions of actin filaments capped by Arp2/3 complex. Eur J Cell Biol *93*, 179-183.
149. von der Ecken, J., Müller, M., Lehman, W., Manstein, D. J., Penczek, P. A., and Raunser, S. (2014). Structure of the F-actin--tropomyosin complex. Nature *519*, 114-117.
150. Wagner, A. R., Luan, Q., Liu, S.-L., and Nolen, B. J. (2013). Dip1 Defines a Class of Arp2/3 Complex Activators that Function without Preformed Actin Filaments. Curr Biol *23*, 1990-1998.
151. Wang, Y., Wu, J., Zsolnay, V., Pollard, T. D., and Voth, G. A. (2024). Mechanism of phosphate release from actin filaments. Proc Natl Acad Sci U S A *121*, e2408156121.
152. Wang, Z., Grange, M., Pospich, S., Wagner, T., Kho, A. L., Gautel, M., and Raunser, S. (2022). Structures from intact myofibrils reveal mechanism of thin filament regulation through nebulin. Science *375*, eabn1934.

 doi:10.20944/preprints202604.2036.v1

153. Wegner, A. (1976). Head to tail polymerization of actin. J Mol Biol *108*, 139-150.
154. Witjes, L., Van Troys, M., Verhasselt, B., and Ampe, C. (2020). Prevalence of Cytoplasmic Actin Mutations in Diffuse Large B-Cell Lymphoma and Multiple Myeloma: A Functional Assessment Based on Actin Three-Dimensional Structures. Int J Mol Sci *21*, 3093.
155. Wriggers, W., and Schulten, K. (1999). Investigating a back door mechanism of actin phosphate release by steered molecular dynamics. Proteins *35*, 262-273.
156. Xu, X. P., Cao, W., Swift, M. F., Pandit, N. G., Huehn, A. E., Sindelar, C. V., De La Cruz, E. M., Hanein, D., and Volkmann, N. (2024). High-resolution yeast actin structures indicate the molecular mechanism of actin filament stiffening by cations. Commun Chem *7*, 164.
157. Xu, X. P., Pokutta, S., Torres, M., Swift, M. F., Hanein, D., Volkmann, N., and Weis, W. I. (2020). Structural basis of αE-catenin-F-actin catch bond behavior. Elife *9*,
158. Yamaguchi, H., and Condeelis, J. (2007). Regulation of the actin cytoskeleton in cancer cell migration and invasion. Biochim Biophys Acta *1773*, 642-652.
159. Yang, S., Huang, F.-K., Huang, J., Chen, S., Jakoncic, J., Leo-Macias, A., Diaz-Avalos, R., Chen, L., Zhang, J. J., and Huang, X.-Y. (2013). Molecular mechanism of fascin function in filopodial formation. J Biol Chem *288*, 274-284.
160. Yuan, B., Scholz, J., Wald, J., Thuenauer, R., Hennell James, R., Ellenberg, I., Windhorst, S., Faix, J., and Marlovits, T. C. (2023). Structural basis for subversion of host cell actin cytoskeleton during Salmonella infection. Sci Adv *9*, eadj5777.